

**Annexure-IX**

**FINAL REPORT OF MAJOR RESEARCH PROJECT**

**Science & Engineering Research Board (SERB)**

**[No. SR/FTP/ES-27/2013, Dated: -20-06-2014]**

**UNDERSTANDING OF ARSENIC PHASE DISTRIBUTION  
AND CO-CONTAMINATION PERSPECTIVE WITH  
FLUORIDE IN THE BRAHMAPUTRA FLOOD PLAINS**



*Submitted by*

**Dr. Ritusmita Goswami, (PI)**

**Dr. Manish Kumar, (Mentor)**

**Department of Environmental science**

**School of Sciences**

**Tezpur Central University, Napaam784028**

**Assam, India**



तेजपुर विश्वविद्यालय / TEZPUR UNIVERSITY

(संसद के अधिनियम द्वारा स्थापित केंद्रीय विश्वविद्यालय)

(A Central University established by an Act of Parliament)

कुल सचिव का कार्यालय/ OFFICE OF THE REGISTRAR

नपाम :: तेजपुर - 784028 :: असम

NAPAAM :: TEZPUR - 784028 :: ASSAM

---

CERTIFICATE

I, Dr. Ritusmita Goswami, declare that the work presented in this report is original and carried throughout independently by me during the complete tenure of major research project funded by Science and Engineering Research Board (SERB), Department of Science and Technology (DST) New Delhi.

**Principle Investigator**

*Ritusmita Goswami*

Dr. Ritusmita Goswami

Assistant Professor,

The Assam Royal Global University, Guwahati, Assam

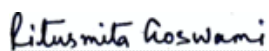
Formerly at Tezpur University, Napaam, Assam

## ACKNOWLEDGEMENT

I would like to express my deep sense of gratitude to Science and Engineering Research Board (SERB), Department of Science and Technology, New Delhi, for the award of project and financial assistance to pursue the research work in the Department of Environmental Science, Tezpur University. My special thanks to my mentor Dr. Manish Kumar, who has guided me throughout the work, has given me the best exposure among the scientific community to present my work and provided all possible support to publish my research work in reputed high impact journals. I am thankful to Tezpur University authorities for providing basic infrastructure facilities in the Department of Environmental Science throughout the tenure of the project. I would like to thank Dr. Arbind Kumar Patel, Ms Dipika Buragohain and Ms. Puspa Changma for helping me in completion of this work.

At the end, I am thankful to almighty for giving me strength and courage to carry out my work.

### Principle Investigator



Dr. Ritusmita Goswami

Assistant Professor,

The Assam Royal Global University, Guwahati, Assam

Former at Tezpur University, Napaam, Assam

1. Title of the project: Understanding of arsenic phase distribution and co-contamination perspective with fluoride in the Brahmaputra flood plains
2. Principal Investigator(s) and Co-Investigator(s): Dr.Ritusmita Goswami (PI)  
Dr.Manish Kumar (Mentor)
3. Implementing Institution(s) and other collaborating Institution(s): Tezpur University
4. Date of commencement: 20.06.2014
5. Planned date of completion: 19.06.2017
6. Actual date of completion: 19.03.2018 (SERB has approved extension for another 9 months)
7. Objectives as stated in the project proposal:
  1. To compare spatial and temporal variation of fluoride and arsenic in the study areas.
  2. To find out the source and possible causes (geogenic or anthropogenic) for the Co-availability of fluoride and arsenic in groundwater.
  3. To simulate water sediment interaction of the study areas in laboratory conditions.
  4. To find out possible mitigation options for As and F
8. Deviation made from original objectives if any, while implementing the project and reasons thereof:No
9. **Experimental work giving full details of experimental set up, methods adopted, data collected supported by necessary table, charts, diagrams & photographs:**

## Content

<b>1</b>	<b>Study area .....</b>	<b>4</b>
1.1	Sampling and laboratory analysis .....	6
1.1.1	BCR Sequential extraction for cation extraction .....	7
1.1.2	Arsenic fractionation.....	8
1.1.3	Sequential extraction.....	8
1.1.4	Calculation of partition coefficient .....	10
1.1.5	Speciation technique .....	10
1.1.6	Batch desorption experiment .....	10
1.2	Statistical analysis .....	11
1.3	Health risk assessment .....	12
1.3.1	Chronic daily intake (CDI) .....	12
1.3.2	Cancer risk (CR) .....	12
1.3.3	Hazard index (HI) .....	13
1.4	Preparation of biochar .....	14
1.4.1	Pyrolysis and activation .....	15
1.4.2	Product characterization.....	15
1.4.3	Adsorption studies .....	16
1.4.4	Adsorption isotherms .....	17
1.5	Experimental design.....	19
<b>2</b>	<b>Results and Discussion.....</b>	<b>20</b>
2.1	Spatial and temporal variation in major ions: .....	20
2.2	Hydrogeochemical facies:.....	22
2.3	Hydrogeochemical processes operating in the aquifers: .....	22
2.4	Weathering, dissolution and ion exchange:.....	24
2.5	Delineating the process of arsenic enrichment:.....	26
2.6	Statistical analysis: .....	27
2.7	Correlation analysis.....	27
2.8	Speciation modelling of the groundwater for arsenic .....	31
2.9	Multivariate statistical analyses .....	33
2.9.1	Principal components analysis.....	33
2.9.2	Hierarchical cluster analysis .....	35

2.10	Speciation modelling of the groundwater for metal .....	37
2.11	Sediment characterization .....	38
2.12	Arsenic fractionation.....	40
2.13	Partition coefficient as a tool to understand “specific mobility” .....	42
2.14	Batch desorption experiment .....	43
2.15	“Operationally defined fractions” of fluoride .....	45
2.16	Co-occurrence and Co-leaching perspective of As and F.....	45
2.17	Biochar characterization .....	46
2.17.1	Proximate and elemental analysis .....	46
2.17.2	Electrical conductivity (EC).....	48
2.17.3	Fourier Transform Infra-red Spectroscopy (FTIR) .....	48
2.17.4	Raman spectroscopy.....	48
2.17.5	Scanning electron microscopy (SEM).....	49
2.17.6	Brunauer–Emmett–Teller (BET) analysis.....	49
2.17.7	X-ray diffraction spectroscopy .....	50
2.17.8	EDX.....	50
2.17.9	Central composite design (CCD) and statistical analysis.....	50
2.17.10	Model validation and response surface plot .....	55
2.17.11	Effect of initial concentration .....	56
2.17.12	Effect of adsorbent dose .....	57
2.17.13	Effect of contact time .....	60
2.17.14	Optimization and validation of result .....	60
2.17.15	Adsorption kinetic study.....	61
2.17.16	Adsorption isotherm .....	62
<b>3</b>	<b>Conclusion.....</b> Error! Bookmark not defined.	
<b>4</b>	<b>Reference.....</b>	<b>70</b>

## List of Figure

<b>Figure 8</b> Map showing the location of Lakhimpur district in India and Assam, the map also shows the sampling location.....	4
<b>Figure 11</b> Piper plot showing the samples of monsoon and post monsoon.....	22
<b>Figure 12</b> Durlov plot showing variation in major ion chemistry monsoon and post monsoon .....	23
<b>Figure 13.</b> Gibbs plot showing that water chemistry of the study area is mainly governed by rock-water interaction. Note. Black dots represent monsoon, while white dots represent post monsoon .....	23
<b>Figure 14</b> Scatter diagram of a) $Tz^+$ versus $Na + K$ , b) $Tz^+$ versus $Ca^{2+} + Mg^{2+}$ , c) $Ca^{2+}/Mg^{2+}$ versus $SO_4^{2-} + HCO_3^-$ d) $SO_4^{2-}$ vs $Ca$ , e) $Cl^-$ vs $Ca^{2+} + Mg^{2+}$ , f) $Na/Cl^-$ vs $EC$ , g) $Cl^-$ vs $Na$ .....	25
<b>Figure 15</b> Scatter plot of a) $As$ and $pH$ , b) $As$ and depth, c) $As$ and $Fe$ , d) $As$ and $PO_4^{3-}$ , e) $As$ and $H_4SiO_4$ , f) $As$ and $SO_4^{2-}$ , g) $As$ and $HCO_3^-$ , h) $As$ and $ORP$ .....	28
<b>Figure 16</b> Saturation index of 14 minerals showing in monsoon for arsenic (n=20) .....	32
<b>Figure 17</b> Saturation index of 14 minerals showing in post monsoon for arsenic (n=20) .....	32
<b>Figure 18.</b> Dendrogram showing the clusters of different water quality parameters during a) monsoon and b) post monsoon of the study .....	35
<b>Figure 19</b> Health risk assessment $As$ exposure through consumption of $As$ contaminated drinking water in terms of hazard index (HI) among children, adult in a) monsoon and b) Post monsoon season.....	37
<b>Figure 21</b> Saturation index of 13 minerals showing in monsoon for metal (n=11)	38
<b>Figure 22</b> Saturation index of 14 minerals showing in post monsoon for meta l (n=20) .....	38

## List of Tables

<b>Table 3</b> Descriptive statistical summary of physiochemical water quality parameter in monsoon and post monsoon. ....	<b>21</b>
<b>Table 4</b> Descriptive statistics for monsoon all units are in mg/L except EC, ORP and As, which have been expressed in $\mu\text{Scm}^{-1}$ , mV and $\mu\text{g/L}$ .....	<b>29</b>
<b>Table 5</b> Descriptive statistics for post monsoon all units are in mg/L except EC, ORP and As, which have been expressed in $\mu\text{Scm}^{-1}$ , mV and $\mu\text{g/L}$ .....	<b>30</b>
<b>Table 6: Multivariate factor analysis score for the monsoon and monsoon period</b> .....	<b>34</b>

## Executive Summary

A study of hydrogeochemical control and mobilization of arsenic was carried out in Lakhimpur district, Assam with the objective of investigate the arsenic contamination status and factor governing its release based on various water types, relation of arsenic with major ions and with various depth profile as well as estimation of age wise health risk due to arsenic intake in drinking water. A total of 126 groundwater samples were collected to represent monsoon and post monsoon season. The processes responsible for arsenic enrichment and origin of groundwater mineralization was determine by calculating saturation index using MINTEQ. Multivariate statistical analysis was done to identify arsenic release mechanism based on rock water interaction. Principle component analysis of physicochemical parameters revealed that the association As with  $\text{SiO}_2$  in monsoon. Main mode of arsenic mobilization of Lakhimpur district is reductive hydrolytic process rather than oxidative process. Reverse ion exchange and ion exchange are governing processes over evaporation and halite dissolution is also a major process in the aquifers. Gibbs plot showed that weathering or rock water interaction was the main hydrogeochemical process operating in the aquifer of Lakhimpur district. Piper plots indicates that good recharge in post monsoon season. Hierarchical cluster analysis reveals that arsenic with Fe-dissolution, phosphate leaching is sources of arsenic. Saturation index of minerals for arsenic indicates water are saturated with goethite,  $\text{FeCO}_3$ , ferrihydrite but other important minerals are under saturated in the aquifer and may leads to increase of arsenic in groundwater by dissolution of minerals in near future in Lakhimpur district and develop into a condition like other highly arsenic affected district such as West Bangal in India and in Bangladesh. Health risk reveals that children are more susceptible to cancer and chances of having non-cancerous health hazards than adults with consumption of arsenic contaminated drinking water. Speciation of metals indicate that Zn, Cd, Ni, Pb concentration are very high except uranium and mostly found as free metal ion in both season. Saturation index of metal indicates that ground water is saturated with goethite,  $\text{FeCO}_3$ , ferrihydrite but other minerals are found in unsaturated condition so there will be cance to increase metal concentration in near future. A futher study was needed to understand the metal toxicity and transport in ground water of Lakhimpur district.

Natural weathering processes were found to have more control on the hydrogeochemistry of the region than anthropogenic activities. The sediment samples were found to be mainly of mixed traced elements  $\text{Na}^+$ ,  $\text{K}^+$ ,  $\text{Ca}^{2+}$ ,  $\text{Mg}^{2+}$ , Cd, Mn, Pb, Zn, Co, Fe, mainly determined by BCR process. Over all reducing conditions were found to be more prevalent, therefore reductive hydrolysis of Fe (hydr)oxides appeared to be the dominant process of As release. This finding was further supported by the correlation observed between As and Fe in the region. Depth seems to govern/influence As hydrogeochemistry but not  $\text{F}^-$  contamination as such. Alkalinity and pH were also found to affect mobilization of As and  $\text{F}^-$ .

Since, there found insignificant correlation between As and  $\text{F}^-$  in the natural conditions, therefore an effort was made to understand the synergistic or the antagonistic dynamics of co-contamination at laboratory scale using sequential extraction procedure (SEP) and batched desorption experiment performed on soil/sediment. Arsenic fractionation was performed on 22 depth wise varying sediment samples collected from the Lakhimpur to understand As phase distribution. The SEP selected for As fractionation extracted 5 “operationally defined” fractions of As. Fraction I and II are regarded as labile phases and are found to be removed or leached through anion exchange with sulphates and phosphates. Fraction III and IV are found to be associated amorphous and crystalline oxides and hydroxides of Fe respectively and together can be called the Fe (hydr)oxides associated As phase. The last or fraction V is regarded as the residual As and is found to be associated with sulphide phases like orpiment ( $\text{As}_2\text{S}_3$ ). The total As extracted from the soil/sediment samples was found to show high positive correlation with the clay. Results of the SEP reveal that out of all the As fractions extracted, fraction II and the Fe (hydr)oxide associated fraction (III+IV) has the highest dependence on clay and organic matter content of the soil/sediments. This shows that breaking, modification and alteration of the functional groups of organic matter could facilitate the release of As from Fe (hydr)oxides. This process is likely to be a microbially mediated step which consumes  $\text{O}_2$  leading to reducing conditions in the groundwater. The previous observations regarding the prevalence of reductive hydrolysis of Fe in the sampling sites along with the findings of the SEP were used to design the batch desorption experiment for studying the co-evolution of As and  $\text{F}^-$  from the soil/sediments.

Batch desorption experiment was designed to observe the leaching of As and F<sup>-</sup> from the soil/sediment samples after spiking with a solution of known As and F<sup>-</sup> concentration at acidic (pH 5) , neutral (pH 7) and alkaline conditions (pH 10). The experiment was conducted at two different conditions, one set of experiment was performed on raw soil/sediment samples, while the other set was conducted after removing the Fe (hydr)oxides from the soil and sediments. The Fe (hydr)oxide fraction was removed from the soil/sediment samples by using a CBD solution (Na-citrate + Na-bicarbonate + Na-dithionite). Leaching of As and F<sup>-</sup> was observed in both sets of soil/sediment samples at acidic and alkaline conditions to observe the role of pH in the desorption mechanism. It was observed that raw soils desorbed much greater amounts of As and F<sup>-</sup> than CBD treated soils. The possible reason could be the involvement of Fe (hydr)oxides. Iron (hydr)oxides coatings on soil and sediment particles are found to have a net positive charge, therefore this phase acts as a very good substrate for adsorption of F<sup>-</sup> and As oxyanions. Removal of Fe (hydr)oxides effectively robs the CBD soil/sediment samples of their ability to complex and adsorb negatively charged species. Since the CBD soil/sediments adsorbed negligible amounts of As and F<sup>-</sup> during the spiking process therefore the amount leached was also very minimal. Over all higher amounts of As and F<sup>-</sup> were found to be released at alkaline conditions. The process of co-contamination can be further studied by the application of techniques like column leaching, multilayer sampling, isotope tracing and Fourier Transform Infrared (FTIR) spectroscopy.

Various mitigation options were also applied to remove these geogenic contaminants from water using biochar prepared from different low cost materials. Efficient removal of both As and F<sup>-</sup> were observed using locally available low cost adsorbents.

**Keyword:** *Arsenic, Fluoride, metal speciation, health risk, chronic daily intake, saturation indices, cluster analysis, mitigation*

## 1 Study area

Lakhimpur has an area of 2277 km<sup>2</sup> and lies between 26°44'00" and 27°53'00" north latitude and 93°42'00" and 94°20'00" east longitude. It is located in north of Siang and Papumpare District of Arunachal Pradesh and east of Dhemaji district and Subansiri River, south of Majuli District and west of Gohpur of Biswanath District. Its major rivers include Brahmaputra, Ranganadi, Dikrang and Subansiri and they are perennial in nature. Main drainage system of this district is controlled by Brahmaputra and Subansiri, Ranganodi and Dikrang river are debouch in Brahmaputra and forming a drainage network. Brahmaputra River and peak discharge observed in monsoon season. Small stream near foot hills are dried up during March and April. The river beds and banks of these rivers consist of boulders, cobalt, pebbles and sand of different grades with very low concentration of clay minerals.

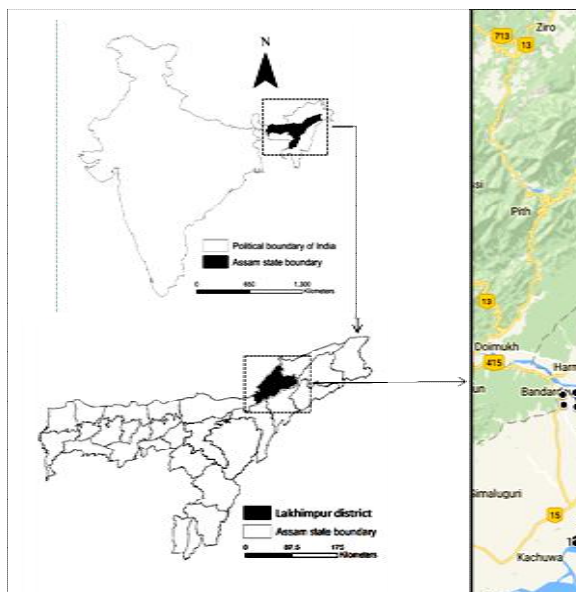


*Figure 1 Map showing the location of Lakhimpur district in India and Assam, the map also shows the sampling location*

Physiographically Lakhimpur District shows three major variations i.e. the hilly tract, the foot hill region the extensive flood plain created by Brahmaputra, Dikrang, Subansiri, Ranganodi river in southern part. Hilly tract consist of Siwalik sediments of lesser Himalayas, foot hill region consist of older terrace deposit. There are two terrace surfaces i.e. Harmoti and Joyhing which represent high and low level terrace respectively and consist of boulders, pebbles of quartzitic and gneissic rocks with fine sand, silt and clay. Lakhimpur district consists of older and newer alluvium deposit. It

includes swampy or marshy land, river terrace, flood plains, points bar, channel bar, river channels and paleochannel. The average altitude of this district (in central and southern flood plain) is varies from 80 to 85 m above mean sea level. General slope of this district is from northern and eastern corner towards southern. Northern limit of flood plain area is marked by 92 meter contours.

Lakhimpur district is divided into two hydrogeological unit i.e. semi consolidated and unconsolidated. In shallow aquifer system water bearing horizons occur within 30 to 50 mbgl and ground water occur into unconfined to semi confined condition. Shallow aquifer materials are different grades of sand with varying proportion of gravels and grain size is decreased towards southern part of district. In entire district semi confining layer is not persistent but thickness is about 3m and top confining layer is composed of clay with interlayer having thickness from varying 15m to 1m. Ground water occur semi confined to confined condition in deeper aquifer. Deeper aquifer materials are consist of different size of sand and gravels and thickness of upper confining layer is 3 to 9 m. Granular zones of deeper aquifers cumulative thickness varies from 60 to 150 m. Grain size of aquifer material are clearly distinct in northern, southern and western part of the district. Narayanpur is deciphered from lithilog and multi aquifer system is present in Dholpur area. In east direction i.e. Panigaon and Dhakuakhana single aquifer zone is found down to depth of 130 mbgl. Direction of groundwater flow of is from higher elevation in north towards in the plain area of south and it flow from northwest to southwest in western part of district. Around Dhakuakhana and Ghilamara area (in central and eastern part) groundwater is flow from north to south. Water table is highest in the floodplain area toward south, it is 110 m above mean sea level. Gradient of flow is higher towards western part compared to eastern part. Water table gradient is steeper (1.5m/km) in northern foot hill and it form recharge zone for entire district. Net groundwater availability of this district is 1198.15 mcm in 2009 (Central groundwater board north eastern region, Ministry of groundwater resource Guwahati).

Climate is subtropical, humid and high rainfall. The average rainfall is 3268 mm, relative humidity 74% to 89%, mean relative humidity is 81%, maximum and minimum temperatures are 35<sup>0</sup>C (June to July) and 8<sup>0</sup>C (December and January) respectively. Highest rainfall occurs on northern part of the district.

### 1.1 Sampling and laboratory analysis

During monsoon (2016) and post monsoon season (2017) groundwater samples are collected (n=126) from Lakhimpur district of Assam. Sampling sites were chosen on the basis of type of land use, aquifer depth and different geological formation. Samples were collected in polypropylene bottles of 500 ml (for analysis of cation and anion) and 125 ml (for analysis of metal). Bottles were washed by groundwater samples for 2-3 times before collecting samples and samples were collected from hand pump or tube wells. Before collecting water samples pumped it for at least 10 min to remove residual water and make sure minimum interference of oxygen. For analysis of arsenic minimum 100 ml sample was filtered by using 0.45  $\mu\text{m}$  Millipore filters and preserved by using  $\text{HNO}_3$ (1:1) to reduce sample pH to 2 and stored it at 4°C. The geographical location of sampling points were collected by using handheld GPS set (Garmin GPS map 76CSX). We measured pH, EC, ORP, TDS, DO of the sample in the sampling site by using HANNA HI9128 multiparameter water quality portable meter. Fluoride is measured in laboratory by using ISE meter (Thermo Fisher Scientific, STARA2140).  $\text{Na}^{2+}$ ,  $\text{Ca}^{2+}$ ,  $\text{K}^+$ ,  $\text{Mg}^{2+}$ , Mn, Fe, Cd, Pb,  $\text{Na}^+$ , Ni, Zn, Co were analyzed by inductively coupled plasma optical emission spectroscopy (ICP-OES, Perkin Elmer Optima DV1000) and As was analysed by atomic absorption spectroscopy (Thermo scientific ICE 3000). Arsenic was analyzed using Atomic Absorption Spectroscopy (AAS, Thermo scientific ICE 3000). Fluoride concentration is measured by ISE-meter (Ion selective electrode meter Thermo fisher scientific, STARA2140). By calculating charged balance ( $\text{Tz}^+ - \text{Tz}^- / \text{Tz}^+ + \text{Tz}^-$ ) analytical method accuracy was checked, where  $\text{Tz}^+$  is total cations and  $\text{Tz}^-$  is total anions, it is calculated in  $\text{meqL}^{-1}$  and charge balance of data is within  $\pm 10\%$ .

Grain size fractionation was done by using sieving technique, a total of 6 sieve grades were used, which were: 4000, 2000, 500, 250, 125 and 63  $\mu\text{m}$ . The sieves were arranged in decreasing order of size and 100 g sample was poured into the largest sieve then mechanically shaken for 10 min. Percentage share of each fraction was found by the following formula: percentage share  $\frac{1}{4}$  (weight of fraction in each sieve/100)  $\times 100$ . Size fractionation was done by comparing the fractions to the size chart given by (*Wentworth, 1922*).

### 1.1.1 BCR Sequential extraction for cation extraction

**Step one:** 40ml of acetic acid 0.11M was added to a 1 g of sludge sample in a 100-ml centrifuge tube, stopper and extracted by shaking for 16 h at room temperature (overnight). No hold-up should occur between the addition of the extractant solution and the beginning of the shaking. The extractant was separated from the solid residue by centrifugation at 3000 rpm for 20 min and the resultant supernatant liquid was transferred into a polyethylene volumetric flask and analyzed immediately. The residue was rinsed by adding 20 ml of distilled water, shaking for 15 min on the shaker and was centrifuged for 20 min at 3000 rpm. The supernatant was decanted and discarded.

**Step two:** 40 ml of a freshly prepared of hydroxylammonium chloride was added to the residue from step 1 in the centrifuge tube, resuspended by manual shaking, and then extracted by mechanical shaking for 16 h at room temperature (overnight). No delay should occur between the addition of the extractant solution and the beginning of the shaking. The extractant was separated from the solid residue by centrifugation and decantation as in step 1. The extract was kept in a polyethylene volumetric flask to be analyzed as before. The residue was washed by adding 20 ml distilled water, shaking for 15 min on the end-over-end shaker and centrifuging for 20 min at 3000 rpm. The supernatant was decanted and discarded.

**Step three:** 10 ml of 8.8 M hydrogen peroxide was carefully added to the residue in the centrifuge tube and digested at room temperature for 1 h with occasional manual shaking. The digestion was continued for 1 h at  $85 \pm 2$  °C, with occasional manual shaking for the first 1/2 h; in a water bath, and then reduced to a volume less than 3 ml by further heating of the uncovered tube. A further aliquot of 10 ml of hydrogen peroxide was added. The tube, with cover, was heated again at  $85 \pm 2$  °C and digested for 1 h with occasional manual shaking for the first 1/2 h. After that, the cover was removed and the volume of liquid was reduced to about 1 ml. Then 50 ml of 1.0 M ammonium acetate was added to the cool moist residue and shaken for 16 h at room temperature (overnight). The extract was separated from the solid residue by centrifugation and decantation as in step 1.

**Step four:** The residue remaining at the end of the step 3 was digested as the same aqua regia digestion.

### 1.1.2 Arsenic fractionation

Fractionation of As was done by using the modified five step sequential extraction procedure (SEP) developed by (*Wenzel et al., 2001; Hamon et al., 2004; Haque et al., 2008*) (Table 3) providing the SEP scheme. The method was validated with the help of standard reference material (SRM) 2710a, which is a soil from Montana, USA with a particle size <74  $\mu\text{m}$ . It is essential to use a certified reference material (CRM), because it can be also helpful for future comparisons.

### 1.1.3 Sequential extraction

Sequential extraction of arsenic was adopted to identify and extract the “operationally defined” fractions of arsenic in the samples. The method adopted for this experiment is the modified sequential extraction procedure (SEP) given by (*Haque et al., 2008; Wenzel et al., 2001; Hamon et al., 2004*). The details of the above experiment have been elaborated in the section below:

Fraction I: In a 50 ml centrifugation tube 1g of dry soil / sediment sample was taken. 25 ml of 0.05 M  $(\text{NH}_4)_2\text{SO}_4$  was added to the centrifuge tube and the mixture was shaken for 4 hr in a mechanical shaker. After this the mixture was centrifuged (Eltek Multispin TC650D) at 2000 rpm for 15 min. The supernatant was separated as extract I, it was acidified with  $\text{HNO}_3$  (2 to 3 drops) and stored in a freezer at 4°C till analysis. The residue that was left was used in the next step.

Fraction II: The residue soil from the 1<sup>st</sup> step was again poured in a 50 ml centrifugation tube. 25 ml  $(\text{NH}_4)_2\text{HPO}_4$  of 0.05M strength was added to the tube and the mixture was shaken for 16 hr at 20 °C. Afterwards the mixture was centrifuged at 2000 rpm for 15 min. The supernatant was separated as extract II, it was acidified with  $\text{HNO}_3$  (2 to 3 drops) and stored in a freezer at 4°C till analysis. The residue that was left was used in the next step.

Fraction III: The residue of the last step was poured in a 50ml centrifugation tube.  $\text{NH}_4^+$ - oxalate buffer (0.2 M) was added to the residue and the pH was adjusted to 3.25 using oxalic acid, the soil solution ratio was 1: 25. The mixture was shaken at 20°C for 4hr in the dark and washed with  $\text{NH}_4^+$  – oxalate (0.2M, pH 3.25) in a soil solution ratio of 1:12.5 for 10 min. The mixture was centrifuged as in the previous steps and the residue was used in the next step, while the supernatant was marked as extract III and

stored till further analysis in a manner described in the previous steps .

Fraction IV: The residue of the last step was again poured in a centrifugation tube.  $\text{NH}_4$ - oxalate buffer (0.2 M) was added to the residue and ascorbic acid (0.1M) was added to adjust the pH to 3.25. *The soil solution ratio was 1:25. The mixture was shaken for 30min in water bath at  $96 \pm 3$  °c* in the light. Later  $\text{NH}_4$ -Oxalate (0.2 M, pH 3.25) was used in the wash step with a soil solution ratio of 1: 12.5 by shaking for 10min.

Fraction V: The residue of the last step was finally digested in a metal digester (Pelican Kelplus Kelvac) by adding 50ml solution of 16N  $\text{HNO}_3$  and 30%  $\text{H}_2\text{O}_2$  or these sediment samples were digested following the  $\text{HNO}_3$  and  $\text{HClO}_4$  digestion method. Accurately weighed amount (1g) of the sample was taken in a Teflon acid bomb. 3.0 ml of nitric acid and 2.0ml of perchloric acid were added to the sample. Then the acid bomb was placed in an oven for heating at 100 °C for eight hours. After digestion, the sample was cooled, filtered and transferred to a 25.0ml volumetric flask. The solution was then made up to 20 ml with the help of distilled water. The sample solutions were then transferred in plastic bottles and preserved in freeze at 4 °C.

**Table 3 :- Outline of the SEP for arsenic fractionation in the soil and sediment samples**

Fraction	Extractant	Wash step	Target phase	Possible mechanisms
I	0.05M $(\text{NH}_4)_2\text{SO}_4$ : 4h shaking , 20 °c		Physisorbed arsenic (outer sphere surface complexes), commonly referred to as labile or reactive arsenic.	Anion exchange of $\text{SO}_4$ for arsenic
III	$\text{NH}_4$ - oxalate buffer (0.2 M): pH 3.25 : 4h shaking in the dark , 20 °c	$\text{NH}_4$ -oxalate buffer (0.2 M): pH 3.25; 10 min shaking in the dark.	Non labile arsenic associated with amorphous and poorly crystallized Fe (Mn, Al) oxides/oxyhydroxides.	Ligand-promoted dissolution.
IV	$\text{NH}_4$ - oxalate buffer (0.2 M) : + ascorbic acid (0.1) c pH 3.25 : 30min in a water bath $96 \pm 3$ °c in the light	$\text{NH}_4$ oxalate buffer (0.2 M): pH 3.25: 10 min shaking in the dark	Non labile arsenic associated with well crystallized Fe (Mn, Al) oxides/ oxyhydroxides.	Reduction of Fe (III) and Al (III)
V	$\text{HNO}_3/\text{H}_2\text{O}_2$ ; Microwave digestion.		Liberated arsenic associated with residual minerals such as orpiment.	Oxidation of sulphides and organic matter

#### 1.1.4 Calculation of partition coefficient

Partition coefficient has been described as the ratio of the quantity or amount of contaminant in the soil/sediment ( $C_T$ , expressed in mg metal per kg sorbing material) to the quantity that has been leached out ( $C_L$ , expressed in mg metal per L of solution) (EPA, 2005), the formula being:

$$K_d = C_T / C_L$$

Two different partition coefficients were calculated in our studies,  $K_{d1}$  (where the sum of fractions I and II was taken as  $C_L$ ) and  $K_{d2}$  (where the groundwater As level of the corresponding sites was considered  $C_L$ ). The calculation of  $K_{d1}$  can be found to be comparative to other relevant studies like Yang *et al.* (2012), in which the partition coefficient was calculated as the total As in the soils divided by the As in the soil solution. In the above mentioned study also the easily leachable fractions of As were found to be responsible for As content in the soil solution. Comparative values of  $K_{d1}$  and  $K_{d2}$  were evaluated and then assessed against other variables by utilizing correlation coefficient to ascertain the trend.

#### 1.1.5 Speciation technique

A minerals SI (saturation index) can be calculated by using this equation (Garrels and Christ 1965).

$$SI = \log^{10}(K_{IAP}/K_{SP})$$

Where SI = Saturation index,  $K_{IAP}$  = Product of particular solid phase ion activity and  $K_{SP}$  is solubility product of phase. Saturation states are considered as saturation (equilibrium;  $SI=0$ ), under saturation (dissolution;  $SI<0$ ) and oversaturation (precipitation;  $SI>0$ ) based on value of SI.

#### 1.1.6 Batch desorption experiment

The experiment was performed on raw samples and (hydr)oxide removed samples at acidic, neutral and alkaline pH (Kim *et al.*, 2012). The schemes of experiments have been elaborated in which were performed on raw (untreated) samples and Fe (hydr)oxides removed samples based on the methodology given by Mehra and Jackson (1960). Fe(hydr)oxide fraction was removed from the soil and sediment

samples by treating 4 g soil with 40 mL of 0.3 M Na-citrate and 5 mL 1 M Na bicarbonate and 0.1 g Na-dithionite (CBD) in a water-bath at 80 °C for 0.5 h. The above procedure was repeated three times to ensure complete removal of the Fe (hydr)oxide fraction, the leachate after CBD treatment was analysed for As and the values were compared with the As values extracted previously by the SEP. Spiking was done on untreated and CBD treated soil/sediment samples by exposure to a standard solution (As 1000 µg/L, F<sup>-</sup> 100 mg/L; 1:10). Sorption was noted for raw and CBD treated samples and desorption was observed under conditions of acidic (pH 5), neutral pH (7) and alkaline pH (pH 10).

**Table 4 : Outline of desorption experiment in the soil and sediment samples .**

Soil pretreatment <b>Raw soils:</b> 4g of raw soil was pulverised and dried at 50°C for leaching. <b>CBD treated soils:</b> Fe (hydr) oxide free soil was prepared by reacting the raw soil (4g) with 40mL of 0.3 M Na-citrate + 5mL. 1M Na-bicarbonate + 1g Na-dithionite (CBD) in a water bath at 80 °C 0.5 h. The treatment was repeated three times to ensure complete removal of Fe (hydr) oxide.			
<b>Spiking :</b> Both the raw and the CBD treated soils were spiked with a solution of known As and F <sup>-</sup> concentrations (Na <sub>2</sub> Has(V)O <sub>4</sub> -7H <sub>2</sub> O-NaF (Himedia chemicals) solution (As 1000 µgL <sup>-1</sup> , F <sup>-</sup> 100 mgL <sup>-1</sup> ; 1:10) .			
Experiment A ( desorption at pH 5)		Experiment B ( desorption at pH 10)	
Leaching was observed in raw samples for 4 hours.	Leaching was observed in CBD treated samples for 4 hours.	Leaching was observed in CBD treated samples for 4 hours.	Leaching was observed in raw samples for 4 hours.
Arsenic and F <sup>-</sup> analyzed by using AAS and Ion selective electrode respectively.			

## 1.2 Statistical analysis

Statistical techniques: All statistical analyses were performed using Statistical Package for Social Sciences version 20 (SPSS 20) software package. Pearson's Correlation analysis, a form of bivariate analysis has been used, along with multivariate techniques like principal components analysis (PCA) and hierarchical cluster analysis (HCA). PCA is a data reducing technique which helps us find interrelationships

between different parameters based on the principal component (PC) loadings. The importance of the PCs can be assessed by the percentage variance of each of them, higher the variance, greater is the significance (Critto et al., 2003). In HCA, the parameters are classified based on their relation; closer grouping implies more similarities, while greater distance mean lesser similarities (Chen and Liu, 2007).

### 1.3 Health risk assessment

By following USEPA guideline a health risk assessment was done (US Environmental Protection Agency) (1989). Objective of health risk assessment is to find out susceptibility to getting cancer among the people who exposed to As contamination drinking water source especially on children and adults. Population are classified into 4 group such as children (5 to 10), youth(11 to 20), Adult(21 to 40) and Elderly(41+). According to USEPA (2009) average body weight is considered as 10 kg for children, 50 kg for youth, adult and elderly respectively for determining health risk. Average water consumption is considered as 2.4 L in children, 3.3 L in youth and 3.7 L in adult and elderly according to nutrient requirements and recommended dietary allowances (Food and Nutrition Board 2004; Grandjean 2005).

#### 1.3.1 Chronic daily intake (CDI)

Chronic daily intake is calculated by using this formula (USEPA,(US Environmental Protection Agency) 1989).

$$\text{CDI(mg/kg/day)}=\text{Total dose(mg)/Body weight(kg)}$$

Total dose is calculated by As concentration multiplied with adequate intake of water. Adequate intake of water is considered as 2.4 L in children, 3.3 L in youth and 3.7 L in adult and elderly according to nutrient requirements and recommended dietary allowances (Food and Nutrition Board 2004; Grandjean 2005).By using this value CDI is calculated and this value are depicted in supplementary tables 1 & 2.

#### 1.3.2 Cancer risk (CR)

Due to oral ingestion of As drinking water lifetime cancer risk assessment was

calculated by this equation (USEPA, (US Environmental Protection Agency) 1989).

$$\text{Cancer risk} = \text{CDI} \times \text{Potency Factor (PF)}$$

where potency factor of As = 1.5 (mg/kg/day) (established by US-EPA, IRIS 2007)

To calculate the risk of cancer associated with exposure to a carcinogen the cancer slope factor (CSF) is used. It is also called as potency factor and cancer risk is calculated by CDI multiplying with potency factor. Confidence limit of a potency factor is 95 % on enhance cancer risk from exposure of lifetime to an agent such as arsenic due to ingestion or inhalation. Potency factor express in units of population proportion/mg of arsenic/kg body weight/day.

### 1.3.3 Hazard index (HI)

This is the index of non carcinogenic toxicity of a substance i.e. arsenic in this case. It can be calculated by following formula:

$$\text{HI} = \text{CDI} / \text{R}_F\text{D}$$

Where CDI= Chronic daily intake, RFD= The reference dose for arsenic (mg/kg/day) i.e.  $3 \times 10^{-4}$ . If HI value is lower than 1 then it is considered as no significant risk of non carcinogenic effects, whereas if cancer risk value is between  $10^{-4}$  and  $10^{-6}$  then carcinogenic risk is acceptable.

### 1.4 Arsenic and Fluoride Mitigation Approaches

The synergistic toxicity effects of both As and F<sup>-</sup> have been elsewhere and posses a real challenge for simultaneous remediation of the elements. Thus there is an urgent need to find a way for remediation of both contaminants from natural water using a cost effective technique to meet the needs of population exposed to contamination of both As and F<sup>-</sup> or either any one thereof.

Keeping these in mind biochars from different plants materials and waste products have been prepared and applied for remediation of As and F<sup>-</sup> and other contaminants from aqueous solution. Biochar prepared from rice husk, an agricultural waste have been prepared and investigated its F<sup>-</sup> removal efficiency. Moreover, removal

potential of activated biochar prepared from a perennial grass was examined under investigating parameters viz; combined effect of initial concentration ( $\text{mgL}^{-1}$ ), adsorbent dose ( $\text{g50 mL}^{-1}$ ) and contact time (minute) on both As and  $\text{F}^-$  removal from aqueous medium using Central Composite design (CCD) in response surface methodology (RSM) by Design Expert Version 10.0.6 (Stat- Ease Inc., MN, USA).

A removal study has also been designed using a novel nanosized biochar derived from rice husk. Our preliminary investigations indicated that rice husk contains plentiful floristic fiber and some functional groups such as hydroxyl, carboxyl and amidogen, etc. which makes adsorption feasible (Xiao et al., 2001).

Therefore, the present work is designed to study the F sorption characteristics of using nanosized rice-husk biochar (NRB) with respect to various physicochemical parameters such as adsorbent dosage, contact time and initial F concentration. Kinetics of the adsorption process has also been investigated

## **1.5 Preparation of biochar**

### **(I) Biochar preparation from perennial grass**

*S. ravannae* grass samples used in this study were collected from a field experiment conducted at North Bank Plain Zone (one of the six Agroclimatic zones in Assam, India) at Tezpur University campus ( $26^{\circ}41/\text{N}$  and  $92^{\circ}50/\text{E}$ ). Above ground part of the biomass was used in the experiments. Samples were washed with distilled water to remove any adhering substance, sun dried and then cut into small pieces (0.5-1.5 cm). After grounding with a high-speed Willy mill (SECOR Scientific Eng. Co) samples were allowed to pass through 0.2 mm sieves (70 meshes) (as per TAPPI sT257 Om-85 methods). Samples were then oven dried and kept in a desiccator for further analysis and experiments.

### **(II) Preparation of Nano Rice Husk Biochar**

Rice husk collected from a local mill was put in a piece of pyrolysis apparatus for heating at  $600^{\circ}\text{C}$  to produce biochar. The biochar thus produced was termed as raw rice-husk biochar (RRB) and this raw biochar was further put to high energy ball milling to reduce the particle size to nano level. Particle size reduction increases surface to volume ratios and gives new properties to particle surfaces which is very desirable

for adsorption processes. The nanosized adsorbent thus produced was studied by batch technique to obtain the equilibrium data and adsorption kinetics. Effects of various parameters such as adsorbent dose, agitation time, particle size and initial F concentration at constant temperature have been investigated.

### 1.5.1 Pyrolysis and activation

About 10 g of the dry biomass sample was taken in a vertical tube fixed-bed alloy reactor (327.80 mm x 25.40 mm) for the pyrolysis experiments. The details of the pyrolysis process can be found elsewhere (Saikia et al.2015). As given by the statistical software, twenty sets of experiments were conducted within the temperature range of (300-550 °C), heating rate (20-60 °C) and nitrogen flow rate (70-250 ml min<sup>-1</sup>). The biochar yield was computed according to Eq.1.

$$\text{Biochar yield (wt\%)} = \frac{\text{Weight of biochar collected (g)}}{\text{Weight of biomass feed (g)}} \times 100 \quad (1)$$

The biochar thus obtained were kept in desiccators for further analysis and experiments. Further activation of the biochar was carried out by following the method as described by Goswami *et al.*, 2016..

### 1.5.2 Product characterization

#### I. Proximate analysis

Moisture, ash and volatile matter content of the biochar and activated biochar sample were determined by ASTM D 3173, ASTM D 3174 and ASTM D 3175 standards, respectively. Fixed carbon was calculated by subtracting the percentages of moisture, ash and volatile matter from 100.

#### II. CHN analysis

Presence of common elements such as C, H, N and S was determined using a Perkin Elmer, 2400 Series-II elemental analyser. O (wt. %) was measured by the difference of C, H, N and ash from 100.

#### III. FTIR analysis

The FTIR spectrum was recorded on a Nicolet IR spectrometer at room temperature (26 ± 2°C) in the spectral range of 4000-400 cm<sup>-1</sup>.

#### IV. *pH analysis*

pH of *S. ravannae* biochars were calculated following the method as described elsewhere (Saikia et al. 2015) by using pH meter (EUTECH pH 510) at room temperature.

#### V. *Analysis of Electrical conductivity (EC)*

Electrical conductivity (EC) was determined by using conductivity meter (Digital TDS/Conductivity Meter MK 509).

#### VI. *Raman spectroscopy*

To describe the crystallization degree of biochars, a Renishaw in Via Raman microscope equipped with 514 nm laser diode and back scattering configuration was used. The Raman spectra in the range of 500–2500  $\text{cm}^{-1}$  were curve-fitted using the Wire Raman software (version 3.4).

#### VII. *SEM- EDAX analysis*

The surface characteristics of the activated biochars were analysed using field emission scanning electron microscopy (SEM) and energy dispersive X-ray spectroscopy (EDAX) JEOL (JSM-6390 LV) microscope with an acceleration voltage of 20 kV. The EDX is helpful in providing rapid qualitative and semi-quantitative analysis of elemental composition with a sampling depth of 1-2 microns.

#### VIII. *BET analysis*

The surface area of the biochar obtained from *S. ravannae* sample was measured using AS-3012 BET surface area analyser.

### **1.5.3 Adsorption studies**

The adsorption isotherms were investigated by the optimum conditions as given by the statistical software (Version 10.0.6, Stat- Ease Inc., MN, USA). Effect of various parameters such as adsorbent dose, initial metal concentration and contact time were evaluated. All chemical reagents used for the experimental purpose were of high purity grades from Sigma Aldirch. Stock solution for As ( $1000 \mu\text{g mL}^{-1}$ ) was prepared from Sigma Aldirch standard, working standards were prepared by serial dilution of stock

with milliQ water. Simultaneously, F<sup>-</sup> stock was prepared by dissolving 2.21 g NaF in 1000 mL of deionized water followed by dilution to the required concentrations. The initial pH of the metal solution was adjusted to 7 by adding 1M HCl or 1 M NaOH. Batch sorption tests for As and F<sup>-</sup> designed by RSM were conducted by mixing certain amounts of adsorbent with 50 mL of metal solution in a 250-mL conical flask, the batch tests were carried out at room temperature (26±2 °C) by a mechanical shaker at 200 rpm for different contact times. The aliquots collected at different time intervals immediately filtered through 0.45 µm membrane filter (Merck). Concentrations of As in the supernatant was determined with an atomic absorption spectrophotometer (Thermo scientific, Spectrometer Model no. iCE 3000 C113500009 v1.30). F<sup>-</sup> was analyzed using an ion selective electrode (Thermo Scientific Orion 4 star Benchtop pH/ISE meter). Finally the amount of metal adsorbed was calculated by using Eq.2 below

$$q_e = \frac{V(C_0 - C_e)}{m} \quad (2)$$

where  $C_0$  and  $C_e$  are the concentrations (mg L<sup>-1</sup>) of initial and remaining As or F<sup>-</sup>, respectively, V is the volume of As or F<sup>-</sup> solution (mL) and m is the weight of the adsorbent.

The removal efficiency of the metal was calculated according to Eq.3

$$\text{Removal efficiency (\%)} = \frac{(C_0 - C_t)}{C_0} \quad (3)$$

#### 1.5.4 Adsorption isotherms

Adsorption isotherm defines the mass-transfer equilibrium between a reservoir and a surface, on which molecules can be adsorbed (Cai et al. 2015). In the present study, isotherm models were used to evaluate the adsorption capacity of adsorbent and to investigate adsorption mechanisms. In order to evaluate the experimental results and adsorption performance, Langmuir and Freundlich models were used in the present investigation.

### I. *Langmuir isotherm*

Langmuir isotherm assumes that the adsorbent surface contains homogeneous binding sites with the identical sorption energies and there is no interaction with the adsorbed molecules [29]. Langmuir model can be expressed by the following equation,

$$q_e = \frac{q_m K_l C_e}{1 + K_l C_e} \quad (4)$$

where  $q_m$  ( $\text{mg g}^{-1}$ ) is the maximum amount of As or  $\text{F}^-$  adsorbed per unit mass of activated biochar and  $K_l$  ( $\text{mg L}^{-1}$ ) is the Langmuir constant related to rate of adsorption.

### II. *Freundlich isotherm*

The Freundlich isotherm model is an empirical equation employed to define heterogeneous systems. It does not indicate a finite uptake capacity of the adsorbent and can thus only be reasonably applied in the low to intermediate adsorbate concentration ranges (Ahmed et al. 2012). The Freundlich equation can be written as,

$$q_e = K_F C_e^{1/n} \quad (6)$$

where  $K_F$  ( $\text{mg g}^{-1}$ ) and  $n$  are Freundlich constants which give a measure of adsorption capacity and adsorption intensity respectively.

### III. *Adsorption kinetics*

The adsorption mechanism of As and  $\text{F}^-$  was studied by using pseudo first order and pseudo second order kinetic models.

### IV. *Pseudo-first-order kinetic model*

The rate constant of adsorption is determined from the pseudo-first-order equation given by Lagergren and Svenska as,

$$\ln(q_e - q_t) = \ln(q_e) - K_1 t \quad (7)$$

where  $q_e$  and  $q_t$  ( $\text{mg g}^{-1}$ ) are the amount of As or  $\text{F}^-$  adsorbed at equilibrium and at time  $t$  (min) respectively and  $K_1$  ( $1/\text{min}$ ) is the adsorption rate constant.

V. *Pseudo-second-order model*

The pseudo-second-order equation based on equilibrium adsorption is expressed as,

$$\frac{t}{q_t} = \frac{1}{K_2 q_e} + \frac{t}{q_e} \quad (8)$$

where  $K_2$  is the rate constant of second-order equation

VI. *Intraparticle diffusion model*

The intraparticle diffusion model based on the theory proposed by Weber and Morris is expressed as,

$$q_t = k_3 t^{1/2} + C \quad (9)$$

### 1.6 Experimental design

In the present investigation, RSM based on central composite design (CCD) method was used with the design expert software (Version 10.0.6, Stat-Ease Inc., MN, USA). The CCD consists of a  $2^n$  factorial runs with  $2n$  axial runs and  $n_c$  center runs. A  $2^3$  CCD with three independent variables (A represents initial concentration in  $\text{mg L}^{-1}$ ; B represents contact time in minutes and C represents adsorbent dose in  $\text{g/50mL}$ ) at five different levels (-1, +1, 0,  $-\alpha$ ,  $+\alpha$ ) was used for the present investigation. The CCD comprised of eight factorial points, six star (axial points) and six replicates at the center points with one response which is removal efficiency (%). Once the experiments were performed, a second-order polynomial model was fitted to each set of experimental data to determine optimal reaction conditions by using Eq.10,

$$Y = \beta_0 + \sum_{i=1}^n \beta_i X_i + \sum_{i=1}^n \beta_{ii} X_i^2 + \sum_{i=1}^n \sum_{j>1}^n \beta_{ij} X_i X_j \quad (10)$$

where Y is the predicted response, n is the number of experiments,  $\beta_0$ ,  $\beta_i$ ,  $\beta_{ii}$ ,  $\beta_{ij}$  are regression coefficients for the constant, linear, quadratic and interaction terms respectively.  $X_i$  and  $X_j$  are the coded independent factors. Both graphical and numerical analysis was done for the final model and the statistical significance of regression coefficients and effects was checked by using analysis of variance (ANOVA). The experimental range and levels of the independent variables for As and F<sup>-</sup> removal are presented in supplementary document 1 and supplementary document 2 respectively.

## 10. Detailed analysis of results indicating contributions made towards increasing the state of knowledge in the subject:

### 2 Results and Discussion

#### 2.1 Spatial and temporal variation in major ions:

Table 3 represents summary of various physicochemical parameters analyzed for ground water of Lakhimpur district. pH range was found to be from 4.8 to 7.2 in monsoon and 5.6 to 7.2 in post monsoon implying a variation of slightly acidic to neutral. In monsoon season EC was ranging from 50 to 671  $\mu\text{S}/\text{cm}$  and in post monsoon ranging from 64 to 510  $\mu\text{S}/\text{cm}$  and higher value of EC in monsoon indicating weathering and dissolution brought by percolating rain water. Higher EC value in monsoon indicate that attribute to evaporative enrichment of salts. In post monsoon standard deviation is higher than monsoon and it indicate more variability in hydrogeochemical processes than monsoon. It is reported that if higher standard deviation in post monsoon and in monsoon EC value is higher than it can be also linked with local variation in point sources, multiple aquifer system, type of soil and other activities related to agriculture in this area(Kumar et al.2015). Same processes were indicated in present study. ORP was ranging from -88.01 to 365 in monsoon and -126 to 111 in post monsoon and found that oxidising and reducing both aquifers are present. ORP value indicated that more dominant aquifer in this area is reducing as compared to oxidising. Reducing condition is slightly less dominant in monsoon and it may be because monsoon sampling was done in beginning in rainy season, so still sufficient air space was present in the aquifer and it lead to occurrence of oxidation. TDS value was higher in post monsoon than monsoon and above permissible limit but in monsoon TDS value was within permissible limit in present study. According to WHO, TDS permissible limit is less than equal to 500  $\text{mgL}^{-1}$  (WHO 1993).  $\text{Na}^+$  and  $\text{K}^+$  ranging from 1.02 – 17.83 and 0.11 – 34.94 in monsoon and 6 – 25.28 and 0.054 – 12.76 in post monsoon respectively. It indicate from monsoon to post monsoon dilution effect of infiltrating water a major factor and it can mask dissolution and weathering of alkali and earth materials like alkaline and same phenomenon observed for level of  $\text{Ca}^{2+}$  and  $\text{Mg}^{2+}$ . Reactive silica is more in post monsoon as compared to monsoon and it may be because of silicate weathering is more prominence in post monsoon.  $\text{HCO}_3^-$  is higher in

monsoon than post monsoon and it may be because of collection of sample was done in the beginning of rainy season and so lowering of the water table. If water table is lower than it promotes rock-water interaction is higher and leading to weathering and dissolution as well as to ion exchange of  $\text{Na}^+$  (solid) and  $\text{Ca}^{2+}$  (liquid) resulting higher  $\text{HCO}_3^-$  in groundwater (Krainov et al.2001). Chloride level was found higher in post monsoon than monsoon.  $\text{F}^-$  is below permissible limit in both seasons.

$\text{SO}_4^{2-}$  is higher in monsoon and may be due to anthropogenic source such as fertilizer and from applying fertilizer it can be leached into ground water through soil, degradation of organic substance from top soil.  $\text{PO}_4^{3-}$  level almost same in both season and it may be due to effect of adsorption of phosphate by soil.

**Table 1** Descriptive statistical summary of physiochemical water quality parameter in monsoon and post monsoon.

Parameter	Monsoon		Post monsoon	
	Range	Avg $\pm$ SD	Range	Avg $\pm$ SD
pH	4.8 – 7.2	6.1 $\pm$ 0.35	5.6 – 7.2	6.36 $\pm$ 0.33
EC	50 – 671	218.5 $\pm$ 95.03	64 – 510	256.56 - 97.42
ORP	-88.01 - 365	18.47 $\pm$ 67.59	-126 - 111	-17.19 $\pm$ 48.48
TDS	51 – 429	137.81 $\pm$ 67.22	100 - 534	192.7 $\pm$ 78.61
DO	1.4 – 8.6	5.7 $\pm$ 1.81	1.1 – 7.8	3.36 $\pm$ 1.48
$\text{Na}^+$	1.02 – 17.83	3.45 $\pm$ 2.9	6 – 25.28	11.98 $\pm$ 4.21
$\text{K}^+$	0.11 – 34.94	5.07 $\pm$ 4.56	0.054 – 12.76	2.3 $\pm$ 2.12
$\text{Ca}^{2+}$	4.52 – 108.9	43.46 $\pm$ 23.52	6.96 – 67.73	28.19 $\pm$ 13.61
$\text{Mg}^{2+}$	0.29 - 42.9	13.49 $\pm$ 8.87	2.56 – 97.6	22.91 $\pm$ 22.25
$\text{H}^4\text{SiO}_4$	0.56 – 4.63	1.36 $\pm$ 0.86	0.87 – 9.07	2.03 $\pm$ 1.53
$\text{HCO}_3^-$	25.36 – 482.41	255.44 $\pm$ 123.69	100 – 450	213.09 $\pm$ 117.16
CL-	1.57 – 106.5	46.97 $\pm$ 19.84	21.3 – 312.4	43.24 $\pm$ 28.95
$\text{SO}_4^{2-}$	0.68 – 108.03	21.57 $\pm$ 17.22	3.6 – 87.53	17.46 $\pm$ 15.53
$\text{PO}_4^{3-}$	0.04 - 1.04	0.26 $\pm$ 0.2	0.08 – 1.01	0.33 $\pm$ 0.22
As	ND – 200.35	37.46 $\pm$ 43.02	ND – 219.8	39.29 $\pm$ 46.24
Fe	0.11 – 103.10	21.16 $\pm$ 19.04	0.073 – 0.87	0.276 $\pm$ 0.163
F-	0.02 – 0.66	0.22 $\pm$ 0.112	0.015 – 0.66	0.22 $\pm$ 0.11
$\text{Mn}^{2+}$	ND – 25.82	1.45 -1.66	0.001 – 8.03	1.44 $\pm$ 1.66
$\text{NO}_3^-$	0.05 – 56.08	7.84 $\pm$ 10.58	0.02 – 2.117	0.55 $\pm$ 0.46
Depth (feet)	15 - 100	38.49 $\pm$ 18.78	15 - 100	38.49 $\pm$ 18.78

## 2.2 Hydrogeochemical facies:

Analysis of general chemistry and special variation of water was done by utilizing Durlov(Durov 1948)and Piper plot. In piper plot (Fig 10) observed that in monsoon among cation the calcium type water is dominant while anion  $\text{HCO}_3^-$ ,  $\text{Cl}^-$  are dominant and exhibiting Ca-Mg-Cl type and Ca- $\text{HCO}_3$  type of water. In post monsoon condition remains the same but a new mixed type of water with equal dominance of  $\text{HCO}_3$ -Cl and Ca-Na has changed that constitute significant part and imply a good recharge. Some water do have Ca-Na-Mg- $\text{HCO}_3$ - $\text{SO}_4$  type of facies.

Durlov plot (Fig 11) exhibit increase in TDS and pH in the post monsoon season that leads to mixed type water facies with demarcated change in cationic complexion of water. Such changes are indicative of cation leaching that not only total dissolved solid but also causes alkalinity that lead to increase in pH.

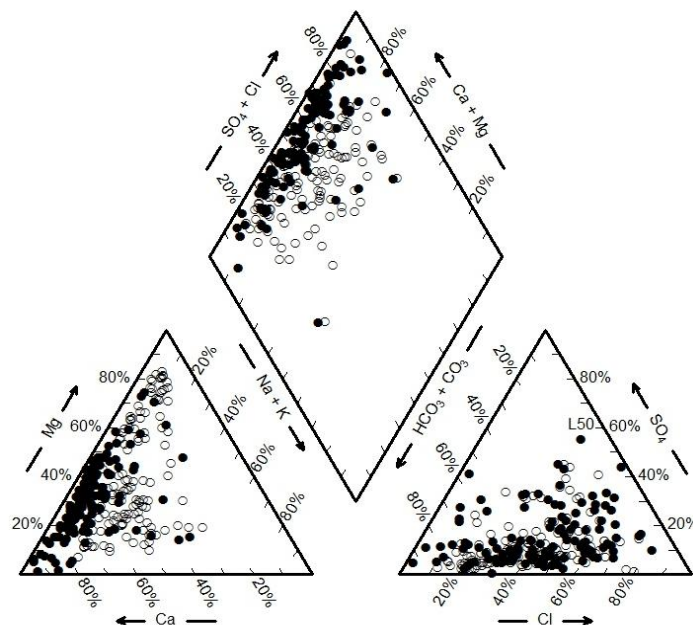


*Figure 2 Piper plot showing the samples of monsoon and post monsoon*

## 2.3 Hydrogeochemical processes operating in the aquifers:

By Gibbs plot examine the preliminary insight into the processes operating in the study area (Gibbs 1970). In present study, it showed that weathering or rock-water interaction was the main hydrogeochemical process operating in the aquifers of Lakhimpur district (Fig12). Therefore, various scatter plots were drawn in the section

given below to understand specific hydrogeochemical processes operating in the study area.

*Note. The black dots and the white dots represent monsoon and post monsoon*

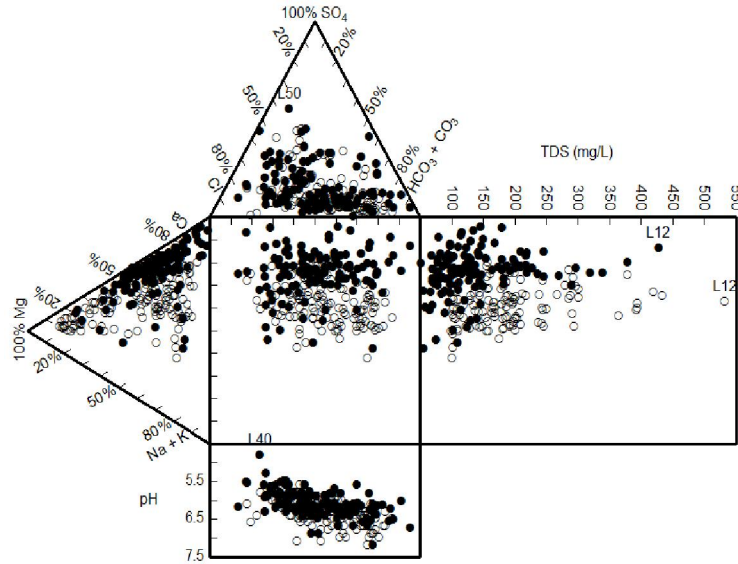


**Figure 3.** Durlov plot showing variation in major ion chemistry monsoon and post monsoon

*Note. Black dots represent monsoon and white dots represent post monsoon samples respectively, while black and hollow triangles represent samples with As levels >10 $\mu$ gL<sup>-1</sup> in monsoon and post monsoon respectively*

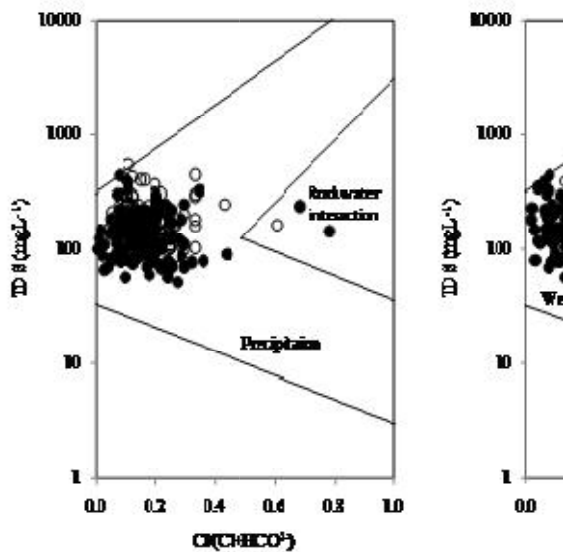


**Figure 4.** Gibbs plot showing that water chemistry of the study area is mainly governed by rock-water interaction. *Note. Black dots represent monsoon, while white dots represent post monsoon*

## 2.4 Weathering, dissolution and ion exchange:

To understand the silicate weathering a plot  $Tz^+$  versus  $Na^+ + K^{2+}$  was drawn and it indicates that most of the samples lie near the 1:0.05 line, indicating that silicate weathering is involved in the geochemical process and Na and K are major ions in groundwater (Fig. 13a).

In a plot of  $Tz$  versus  $Ca^{2+} + Mg^{2+}$  indicates that dolomite dissolution is the dominant process in both seasons because samples lie on the 1:1 line. If samples are close to the 2:1 line, then it indicates that weathering is the dominant process and if they lie above the 1:1 line, it indicates calcite dominance in the aquifer (Maya and Loucks 1995; Kumar et al. 2009) (Fig. 13b).

To ensure the occurrence of carbonate weathering ( $Ca^{2+} + Mg^{2+}$ ) versus ( $SO_4^{2-} + HCO_3^-$ ) a plot was drawn (Fig. 13c). If plots lie close to the 1:1 line, then it can be considered that calcite, gypsum, and dolomite are important sources of  $Ca^{2+}$  and  $Mg^{2+}$ . If points are shifted towards the right, then it indicates that ion exchange was dominant and if points are shifted towards the left, then an opposite trend will be observed, which leads to an excess of  $Ca^{2+}$  and  $Mg^{2+}$  over  $SO_4^{2-}$  and  $HCO_3^-$  (Cerling et al. 1989; Fisher and Multican 1997). In the present study, it was seen that in monsoon and post monsoon, most of the samples are shifted towards the right, indicating that ion exchange and silicate weathering are the dominant processes (Kumar et al. 2006). In monsoon and post monsoon, some points are on the left of the 1:1 line, indicating reverse ion exchange and carbonate weathering, but to some extent, some points lie on the line, indicating that dissolution of calcite, gypsum, and dolomite are sources of  $Ca^{2+}$  and  $Mg^{2+}$  in the system.

The plot  $SO_4^{2-}$  versus  $Ca^{2+}$  shows that most of the samples lie below the 1:2 line and some samples also lie along and above the 1:1 line, except for a few samples in both seasons. It indicates that calcite weathering is the dominant process in the presence of sulphuric acid rather than dolomite (Fig. 13d) (Kumar et al. 2009).

To understand the calcite contribution,  $Cl^-$  versus  $Ca^{2+} + Mg^{2+}$  plots were drawn and they show that Ca and Mg were not increased with salinity, but some samples show an increase with salinity. So, it indicates that reverse ion exchange and ion exchange in clay or weathered layers (Fig. 13e).

It is reported that if evaporation is a dominant process, then it is assumed that mineral species are not precipitated and the  $Na^+/Cl^-$  ratio is unchanged (Jankowski and

Acworth 1997, Kumar et al. 2009). To understand concentration of species due to evaporation and evapotranspiration, a plot  $\text{Na}^+/\text{Cl}^-$  versus EC was drawn. A horizontal 1:1 line was also drawn and clearly observed that samples having  $\text{Na}^+/\text{Cl}^-$  molar ratio are lies below 1:1 line and it indicate that halite dissolution is the major processes in both season and leaching of  $\text{Cl}^-$  in water and it may because of irrigational return flow (Fig.13 f). In  $\text{Cl}^-$  versus  $\text{Na}^+$  plot all samples lies above 1:1 line and indicated that silicate weathering and ion exchange are dominant process and silicate weathering attributed excess of  $\text{Na}^+$ . Few of samples are lied on 1:1 line indicating halite dissolution (fig 13g) Stallard and Edmond 1983, Kumar et al. 2009)

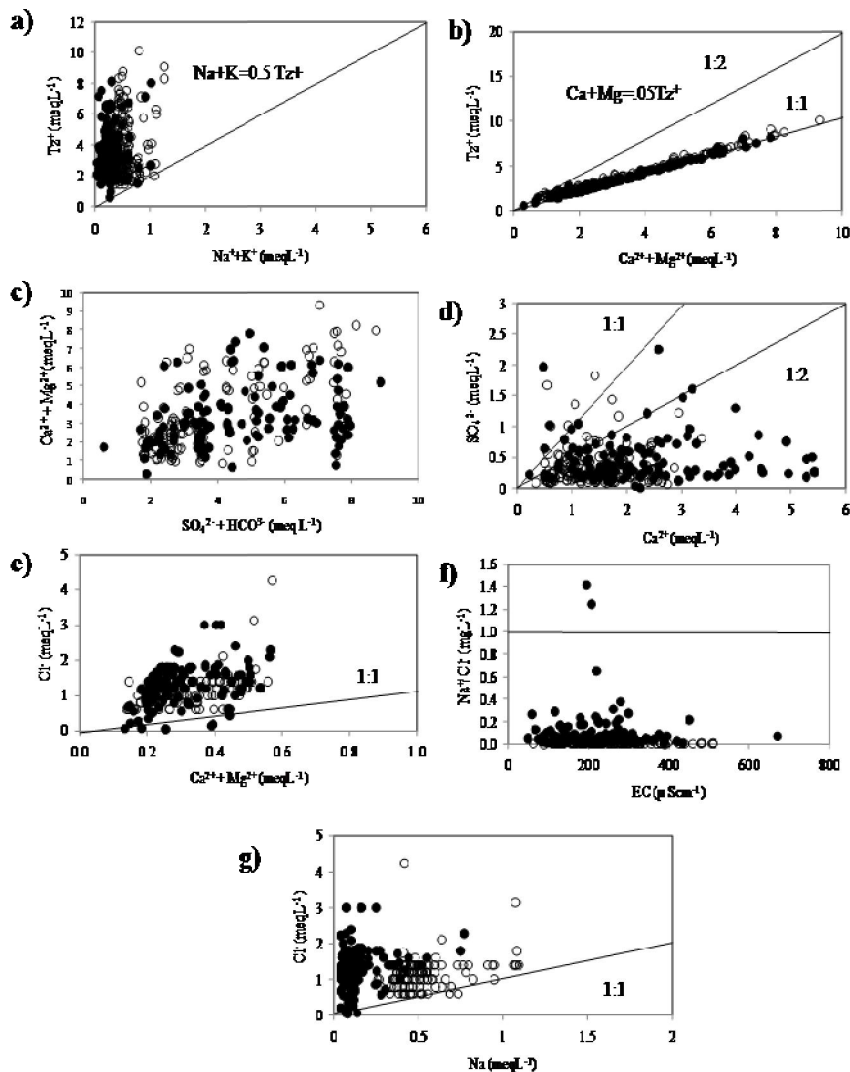


Figure 5 Scatter diagram of a)  $\text{Tz}^+$  versus  $\text{Na} + \text{K}$ , b)  $\text{Tz}^+$  versus  $\text{Ca}^{2+} + \text{Mg}^{2+}$ , c)  $\text{Ca}^{2+}/\text{Mg}^{2+}$  versus  $\text{SO}_4^{2-} + \text{HCO}_3^-$  d)  $\text{SO}_4^{2-}$  vs  $\text{Ca}$ , e)  $\text{Cl}^-$  vs  $\text{Ca}^{2+} + \text{Mg}^{2+}$ , f)  $\text{Na}^+/\text{Cl}^-$  vs EC, g)  $\text{Cl}^-$  vs  $\text{Na}$

Note. Black dots represent monsoon, while white dots represent post monsoon

## 2.5 Delineating the process of arsenic enrichment:

If pH is increased then decrease As adsorption capacity to different substrates like Fe (hydr)-oxides due to higher net negative charge appears and so it repels the negative charged oxyanions (Kim et al. 2012a, b), so high pH leads to mobilization of As. In this study showed same phenomenon that higher the pH seems to favour of As release in groundwater of the study area in both seasons and a definite trend was observed between pH and As. In the pH range between 5.5 to 7.5 high concentration of As was observed. Because of degradation of organic matter pH can rise. In post monsoon highest concentration of As observed in pH 6 and 6.8 and in monsoon highest concentration of As observed in 5.6, 5.8 and 6.5 (Fig.14 a).

To find out the depth distribution of As the plot of depth with As was prepared and As was found to be predominant in shallow aquifers between 20 to 70 feet (Fig.14 b) Depth showed inverse relation with As in the plot Fig b. It is because As is precipitated with increased depth and it may be suitable environment with increasing depth for precipitation of As in the form of arsenopyrite.

In order to investigate the role of Fe, the As vs Fe graph was plotted and observed that relationship between As and Fe was not found (Fig.14c). Many research reported that strong relationship between Fe and As (Kinniburgh and Smedley 2001), As release associated with reductive dissolution of Fe(hydro)oxides (Bhattacharjya et al.1997; Smedley and Kinniburgh 2002; Brahmanet al. 2013; Das et al. 2016). In present study it was not found, so reductive dissolution of Fe(hydro)oxides is not the process of mobilization of As. This may be because of non conservative nature of Fe in ground water due to microbial activity (Kumar et al. 2010b).

As and  $\text{PO}_4^{3-}$  have strong relationship if their source is anthropogenic. Mobility of As in ground water is increased when phosphate fertilizer is used (Katsoyiannis et al. 2008). In present study this was not observed because it may be  $\text{PO}_4^{3-}$  is highly absorbed by soil although it is applied as a fertilizer in agricultural field (Fig.14 d). In present study As and silica show a positive relationship in both monsoon and post monsoon season. But in post monsoon it showed high As concentration with increased silica more than monsoon season (Fig.14e). It is reported that high As water also rich of

silicate (Smedley and Kinniburgh 2002). In post monsoon season As and silica showed strong relationship then monsoon.

Another pathway of arsenic release in ground water is oxidation of arsenic bearing sulphides such as arsenopyrites and pyrite. If this pathway is prevalent in the aquifers than between  $\text{SO}_4^{2-}$  and As, a positive correlation should be observed. But in present study was not found a positive relation between  $\text{SO}_4^{2-}$  and As (Fig.14f). Therefore main mode of As mobilization is reductive hydrolytic process rather than oxidative process in the Lakhimpur District.

In present study it was found that As levels were increased with  $\text{HCO}_3^-$  and it is more clearly indicated in post monsoon than monsoon (Fig 14g).

In mobilization of As, redox potential of the aquifer plays an important role (Smedley and Kinniburgh 2002; Kumar et al.2010). In post monsoon season the plot of As vs ORP shows that As level increased with reducing condition. In monsoon same condition was not observed clearly (Fig14h).

## 2.6 Statistical analysis:

### 2.6.1 Correlation analysis

A correlation analysis is a bivariate method and it is applied to describe the degree of relation between two hydrochemical parameters. The result of the correlation analysis is considered in the subsequent interpretation. Correlation coefficient is if near 1 or -1 then means a good relationship between two variables and if its value is around zero that means no relationship between them at a significant level of  $p < 0.05$  (Kumar et al., 2010). Parameters showing  $r > 0.7$  are considered to be strongly correlated whereas  $r$  between 0.5 and 0.7 shows moderate correlation. In present study, the relationship between various parameters has been studied using Spearman rank coefficient which is based on the ranking of the data and not their absolute values. Resultant matrix showed that negative correlation of pH with most of the variables. It is observed that strong correlation EC with TDS and Ca in monsoon (Table 4). The major exchangeable ion Na-

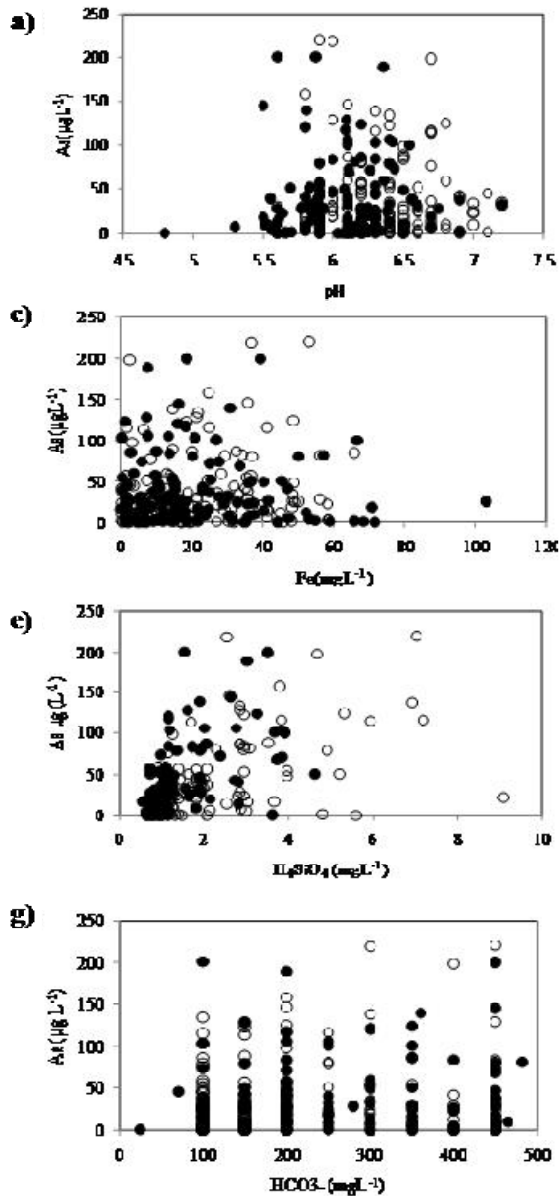


**Figure 6** Scatter plot of a) As and pH, b) As and depth, c) As and Fe, d) As and  $\text{PO}_4^{3-}$ , e) As and  $\text{H}_4\text{SiO}_4$ , f) As and  $\text{SO}_4^{2-}$ , g) As and  $\text{HCO}_3^-$ , h) As and ORP

**Note.** Black dots represent monsoon, while white dots represent post monsoon

Ca correlate positively but Na-Mg correlate negatively in monsoon. In post monsoon the major exchangeable ion Na-Ca and Na-Mg both correlate negatively (Table 5). From observing correlation coefficient in both seasons it can be concluded that the concurrent increase or decrease in the cations is the result mainly of dissolution or precipitation reaction and concentration effects.

Parameters	Depth (feet)	pH	EC	TDS	DO	Ca	K	Mg	Na	Cl	SO <sub>4</sub>	PO <sub>4</sub>	HCO <sub>3</sub>	H <sub>3</sub> SiO <sub>4</sub>	ORP	As	NO <sub>3</sub>	F	Mn	
<b>pH</b>	0.12	1																		
<b>EC</b>	-0.13	0.17	1																	
<b>TDS</b>	-0.11	0.17	<b>0.84</b>	1																
<b>DO</b>	0.03	0.07	-0.06	0.02	1															
<b>Ca</b>	-0.05	0.19	<b>0.60</b>	<b>0.51</b>	0.03	1														
<b>K</b>	-0.04	-0.16	0.00	-0.10	0.00	0.10	1													
<b>Mg</b>	0.11	0.05	0.29	0.40	0.03	0.30	0.00	1												
<b>Na</b>	0.08	0.20	0.01	-0.04	0.03	0.06	0.07	-0.05	1											
<b>Cl</b>	0.11	-0.03	0.07	0.16	0.08	0.14	0.10	0.14	0.21	1										
<b>SO<sub>4</sub></b>	-0.01	-0.11	0.10	0.13	0.20	0.06	-0.13	0.09	0.00	0.03	1									
<b>PO<sub>4</sub></b>	-0.03	-0.03	0.03	-0.12	-0.15	0.05	0.09	-0.05	0.08	-0.12	-0.01	1								
<b>HCO<sub>3</sub></b>	0.05	0.02	-0.49	-0.41	0.01	0.24	0.25	0.19	0.09	0.01	-0.23	0.04	1							
<b>H<sub>3</sub>SiO<sub>4</sub></b>	0.06	0.05	0.00	0.07	0.11	0.01	0.03	0.09	0.07	0.07	0.09	0.01	0.03	1						
<b>ORP</b>	-0.01	0.03	0.12	0.07	-0.01	0.12	0.14	0.09	0.21	0.03	0.10	0.05	0.04	-0.02	1					
<b>As</b>	-0.03	0.00	-0.03	-0.07	-0.02	0.02	0.09	-0.02	0.12	0.08	0.02	0.14	0.07	0.57	0.08	1				
<b>NO<sub>3</sub></b>	0.09	-0.14	0.00	0.19	0.10	-0.11	0.04	-0.02	-0.04	0.18	0.15	-0.12	-0.22	0.07	0.03	-0.08	1			
<b>F</b>	-0.08	-0.01	0.01	0.10	0.12	0.10	-0.07	0.11	0.07	-0.04	0.05	-0.18	0.11	-0.04	0.12	0.01	-0.05	1		
<b>Mn</b>	-0.13	-0.06	0.05	-0.06	0.01	0.10	0.09	0.07	0.21	0.08	-0.01	0.01	0.10	0.07	0.06	0.19	-0.08	0.04		
<b>Fe</b>	-0.06	-0.23	-0.05	-0.12	-0.08	-0.07	0.05	-0.08	-0.11	-0.17	-0.06	0.19	0.01	0.08	-0.09	-0.03	0.03	-0.25	0.13	

*Table 2 Descriptive statistics for monsoon all units are in mg/L except EC, ORP and As, which have been expressed in  $\mu\text{Scm}^{-1}$ , mV and  $\mu\text{g/L}$*

Table 3 Descriptive statistics for post monsoon all units are in mg/L except EC, ORP and As, which have been expressed in  $\mu\text{Scm}^{-1}$ , mV and  $\mu\text{g/L}$ 

Parameter	Depth (feet)	PH	EC	DO	TDS	Ca	K	Mg	Na	SO4	PO4	Cl	HCO <sub>3</sub>	H <sub>3</sub> SiO <sub>4</sub>	NO <sub>3</sub>	F	As	ORP	Mn	Fe	
PH	0.07	1																			
EC	-0.14	0.15	1																		
DO	-0.02	0.22	-0.09	1																	
TDS	-0.03	0.14	<b>0.60</b>	-0.05	1																
Ca	-0.07	0.10	<b>0.73</b>	-0.12	0.32	1															
K	-0.03	-0.07	-0.08	0.05	-0.17	0.02	1														
Mg	0.18	0.07	0.10	0.12	0.18	0.09	0.06	1													
Na	0.04	0.11	0.21	0.12	0.02	0.10	-0.05	-0.07	1												
SO4	-0.01	-0.07	0.14	0.08	0.19	0.09	-0.10	0.09	0.13	1											
PO4	-0.02	0.03	0.03	0.01	-0.16	-0.03	0.03	-0.11	0.07	-0.02	1										
Cl	0.01	0.02	0.01	0.10	0.03	0.21	0.02	-0.06	0.09	-0.01	-0.09	1									
HCO <sub>3</sub>	0.20	-0.01	-0.46	0.10	-0.28	-0.15	0.16	0.71	-0.11	-0.17	-0.06	-0.09	1								
H <sub>3</sub> SiO <sub>4</sub>	0.06	0.08	0.08	0.01	0.20	0.07	-0.01	0.25	0.06	0.15	0.04	-0.09	0.18	1							
NO <sub>3</sub>	-0.03	-0.10	0.08	-0.05	0.05	0.00	0.05	-0.07	-0.09	-0.03	0.00	0.00	-0.10	0.01	1						
F	-0.08	0.00	-0.05	-0.03	0.06	0.02	-0.06	-0.06	0.01	0.03	-0.19	0.00	0.01	-0.07	0.15	1					
As	-0.03	-0.05	-0.08	-0.03	-0.02	-0.03	0.02	0.03	0.13	0.01	0.07	-0.04	0.13	0.56	0.01	-0.01	1				
ORP	0.09	0.00	-0.03	0.13	0.03	-0.03	-0.02	0.19	0.04	-0.06	-0.18	-0.13	0.18	-0.34	-0.20	0.03	-0.55	1			
Mn	-0.10	0.02	0.34	-0.22	0.31	0.27	-0.10	0.05	0.05	0.15	-0.07	-0.02	-0.12	0.07	0.05	-0.01	0.03	-0.12	1		
Fe	-0.10	-0.19	0.06	-0.19	0.09	-0.05	0.03	0.04	-0.02	0.05	0.13	-0.06	-0.04	0.24	0.08	-0.17	0.14	-0.31	0.05	1	
F	-0.06	0.02	0.16	-0.04	-0.01	0.27	-0.05	0.01	-0.07	-0.12	-0.09	0.07	0.01	-0.08	0.01	0.59	-0.13	0.11	0.27	-0.16	

## 2.7 Speciation modelling of the groundwater for arsenic

For speciation modelling to confirm the possibility of solubility control for As total 14 minerals are selected. Selected minerals are  $As_2O_5$ , aragonite, brucite, calcite, dolomite(ordered), dolomite (disorderd),  $FeCO_3$ , ferrihydrite (aged) fluorite, goethite, gypsum, halite, mirabolite, NaF. In monsoon season results shows that samples are super saturated with goethite,  $FeCO_3$ , ferrihydrite. In one sample  $FeCO_3$ , ferrihydrite are in equilibrium.  $As_2O_5$  is very low and highly under saturated (Fig.15). Aragonite, brucite, calcite, dolomite(ordered), dolomite (disorderd), fluorite, gypsum, halite, mirabolite, NaF are also undersaturated in most samples. Only in one sample, halite and fluorite are super saturated. Saturation with goethite indicated that sink for dissolved ion.

The variation in the range of saturation indices of each minerals are almost same in both post monsoon and monsoon season. This is because of collection of samples in monsoon season is in the begining of rainy days. Generally in monsoon season satuartion indices is higher due to good recharge and good recharge change in the environment of the aquifer with redox potential and weathering condition. In post monsoon also samples are super saturated with goethite,  $FeCO_3$ , ferrihydrite but half of the samples are under saturated with  $FeCO_3$ . In post monsoon also aragonite, brucite, calcite, dolomite(ordered), dolomite (disorderd), fluorite, gypsum, halite, mirabolite, NaF and  $As_2O_5$  are under saturated (Fig 16). It indicate that in both season most of the minerals are under saturated except three mineerals and it indicated that there may be increase of aragonite, brucite, calcite, dolomite(ordered), dolomite (disorderd), fluorite, gypsum, halite, mirabolite, NaF and  $As_2O_5$  saturation in near future and will increase arsenic and other groundwater quality parameter.  $As_2O_5$  is highly under saturated in both season, so there may be high possibility to increase arsenic concentration in groundwater. Therefore arsenic in groundwater of Lakhimpur district will increase in near future to develop into a condition like other highly arsenic affected district such as West Bangal in India and in Bangladesh.

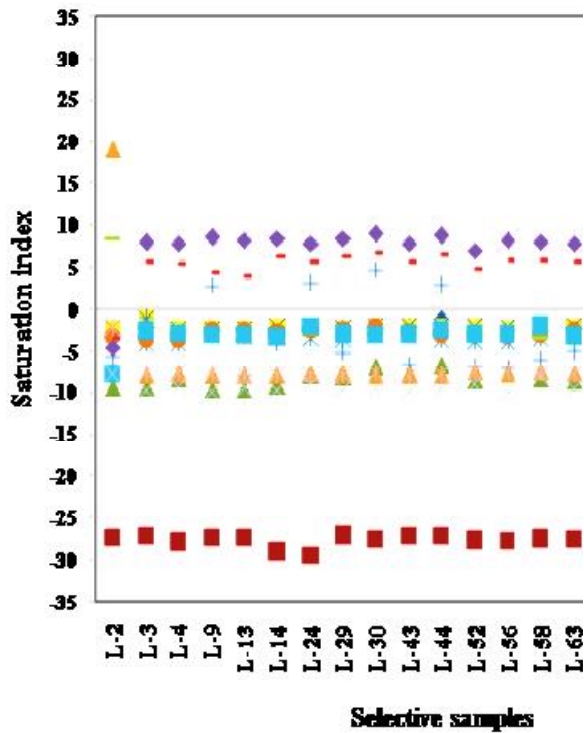


Figure 7 Saturation index of 14 minerals showing in monsoon for arsenic (n=20)

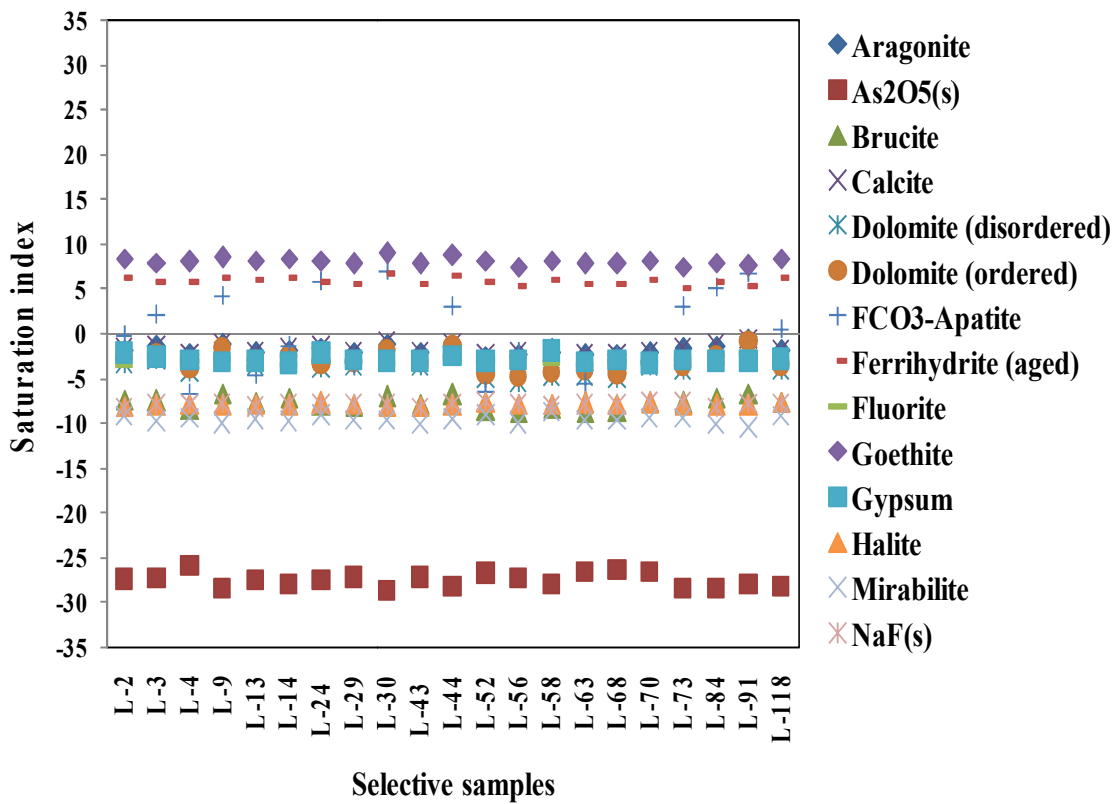


Figure 8 Saturation index of 14 minerals showing in post monsoon for arsenic (n=20)

## 2.8 Multivariate statistical analyses

Previous section is mainly deal with bivariate analysis of different parameters but these technique are less useful when consider the effect of more than one parameter. So multivariate statistical technique was applied to delineate the valuable information on the degree on any interrelationship among the group of variables.

### 2.8.1 Principal components analysis

In present study principal components analysis (PCA) was used with R mode and varimax rotation and obtain 5 principal components (PCs) in both monsoon and post monsoon seasons (Table 6). In monsoon PC1 had 14.07 variance and high loading of EC, TDS and medium loading of Ca, representing ions enrichment specially Ca and more or less dominance of carbonate (dolomite) weathering. PC2 had a variance of 10.01 and medium loading of pH and  $F^{-1}$  representing pH-induced ion exchange specially  $F^{-}$ . PC3 had a variance of 8.31 represented by As and silica and silicate weathering is the controlling process and act as a source of As release in ground water. PC4 had a variance of 8.15 and represented by medium load of K and  $HCO_3^{-}$  which indicate that carbonate weathering and dissolution of minerals like polyhalite in ground water.  $NO_3^{-}$  and  $SO_4^{2-}$  are account for positive loading in PC5 indicating oxidation of sulphide and anthropogenic influences.

In post monsoon variance of PC1 was 13.95 and representing EC, DO, Ca. It indicated that enrichment of ions, fresh water infiltration with higher DO and dissolution of polyhalite mineral. Ca also may be increased in groundwater by agricultural limiting. PC2 represented  $NO_3^{-}$ ,  $SiO_2$  and had a variance of 11.08, it may due to anthropogenic influences and silicate weathering. PC3 had a variance of 10 and high loading of Mg,  $HCO_3^{-}$  showed that carbonate weathering in ground water. pH and TDS are accounting for positive loading on PC4 which indicate pH-induced ion exchange. Variance of PC5 is 6.47 and only accounts  $SO_4^{2-}$  representing oxidation of sulphite in groundwater.

Table 4: Multivariate factor analysis score for the monsoon and monsoon period

Parameter	Monsoon					Post monsoon				
	PC1	PC2	PC3	PC4	PC5	PC1	PC2	PC3	PC4	PC5
Depth (feet)	-.15	.37	.15	-.13		-.12	-.05	.27	.02	.13
pH	.26	.43	.24	-.36	-.44	.22	.06	-.01	.71	.01
EC	.93	-.16		-.14		.91	-.04	-.12	.10	.12
TDS	.89			-.16	.24	-.23	-.08	.12	.76	.003
DO		.38			.35	.72	.01	.03	.12	-.11
Ca	.74			.31	-.20	.78	-.004	.05	-.01	.003
K		-.17		.64		-.10	-.017	.28	-.01	.16
Mg	.48	.21		.28		.16	.013	.90	.08	.010
Na		.30	.39	.18	-.15	.12	.15	-.15	.19	.06
Cl	.14	.29	.17	.28	.35	.13	.05	-.02	-.02	-.03
SO4	.13		.11		.51	-.07	.13	-.20	.14	.67
PO4		-.46	.24		-.32	.05	.01	-.09	.03	-.08
HCO3	-.28	.26		.64	-.43	-.32	.09	.85	-.01	-.08
SiO2			.79		.19	.15	.74	.30	.10	.07
ORP	.19	.13		.32		.06	.12	-.13	.03	-.09
As			.81	.13		-.01	.05	-.10	.06	-.77
NO3					.71	-.08	.88	.06	-.04	-.04
F		.46	-.15	.18		-.01	-.76	.28	.09	-.12
Mn		-.14	.25	.44		.55	.11	-.03	-.29	-.11
Fe	-.13	-.67		.12		.06	.30	.03	-.34	.43
Eigen values	2.82	2.00	1.66	1.63	1.36	2.79	2.22	2.00	1.49	1.29
% of variance	14.07	10.01	8.31	8.15	6.82	13.95	11.08	10.00	7.45	6.47
Cumulative %	14.07	24.08	32.39	40.54	47.36	13.95	25.03	35.03	42.48	48.96
Process	Ion enrichment, carbonate weathering	pH- induced ion exchange	Silicate weathering	Carbonate weathering	Oxidation of sulphite, anthropogenic influences	Enrichment of ion, dissolution of polyhalite	Anthropogenic influences, silicate weathering	Carbonate weathering	pH- induced ion exchange	Oxidation of sulphite

## 2.8.2 Hierarchical cluster analysis

Hierarchical cluster analysis (HCA) was used to similarity and difference between different water quality parameter. Wards method with squared Euclidean distance was used to perform HCA. In this study monsoon has two prominent (Fig.17). Three most significant clustering from the dendrogram are EC-TDS-Ca-Mg, DO-SO<sub>4</sub>-Cl-NO<sub>3</sub>- and SO<sub>4</sub>-As-PO<sub>4</sub>—Fe. EC-TDS-Ca-Mg indicates carbonate weathering contributing ions in water, DO-SO<sub>4</sub>-Cl-NO<sub>3</sub>- indicates that enhanced microbial activity as well as recharge to fluctuate or co-rawation or close linkage between these. Those parameter are recharge sensitive. SO<sub>4</sub>-As-PO<sub>4</sub>—Fe indicated that finally in monsoon As with Fe-dissolution, phosphate leaching sources of As and microbial oxidation. As bearing pyrite rocks leading to SO<sub>4</sub><sup>2-</sup> generation. In post monsoon, most prominent processes are SiO<sub>2</sub>-NO<sub>3</sub>—SO<sub>4</sub>-Fe, pH-TDs-Na-Cl and ORP-As-K-PO<sub>4</sub>. SiO<sub>2</sub>-NO<sub>3</sub>—SO<sub>4</sub>-Fe indicate silicate weathering and microbial activity, anthropogenic, pH-TDs-Na-Cl indicated that pH based on halite dissolution and ORP-As-K-PO<sub>4</sub> indicated that change in redox condition leading to As release and nutrient related control indicative of bio leaching of As rather physical and chemical weathering (Fig.17).

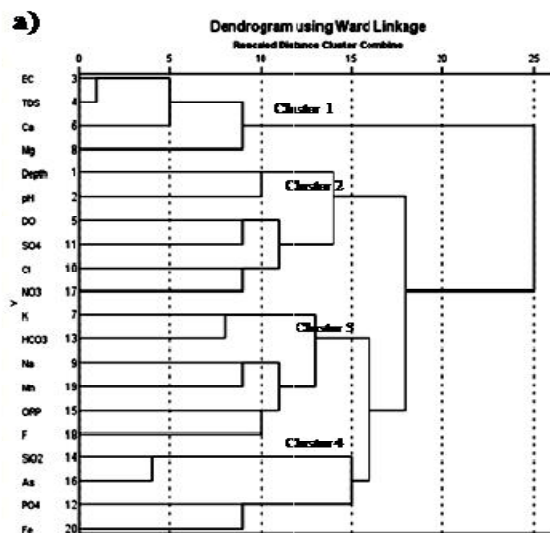
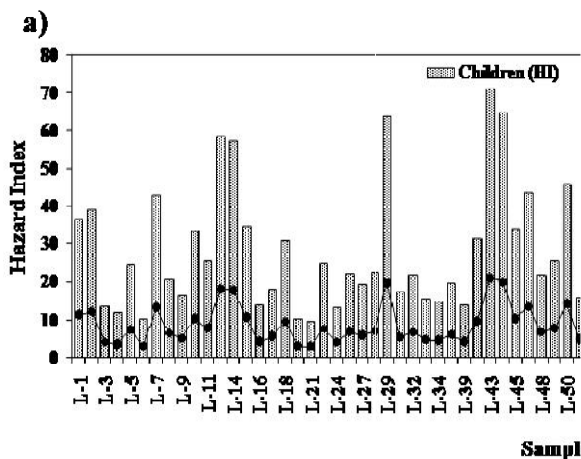


Figure 9. Dendrogram showing the clusters of different water quality parameters during a) monsoon and b) post monsoon of the study

**2.9 Health risk assessment through estimating hazard indices:**

Health risk assessment was done by calculating hazard indices (HI values). The hazard value calculated for present study showed that due to consumption of arsenic contaminated drinking water, the residents in Lakhimpur district higher HI value were found. It was ranging from 8.16 to 70.95 (n=80; considering those sample beyond WHO limit of As) in case of children, while in adult HI value was found ranging from 2.52 to 21.31 (n=80; considering those sample beyond WHO limit of As) in monsoon season (Fig.18a). In post monsoon season children HI value ranging from 10.28 to 78.38 and in adult HI value ranging from 3.17 to 24.17 (n=80; considering those sample beyond WHO limit of As) (Fig.18b). In both season it was found that HI values were much higher than the unit value (HI>1) which is considered for estimating cancer risk for children and adult. It indicates that resident of Lakhimpur district, which are exposed to As contamination they are at high risk of cancer in near future and together with prone to severe non carcinogenic health impacts. During monsoon and post monsoon 100% children and adults both are under high risk cancer as per estimation of HI values.

Overall, it was found that children are more susceptible to cancer risk together with non-carcinogenic health impacts than adults in both season (Fig.18a and b) Difference between the cancer risk among children and adult are clear from (Fig.18a and b).



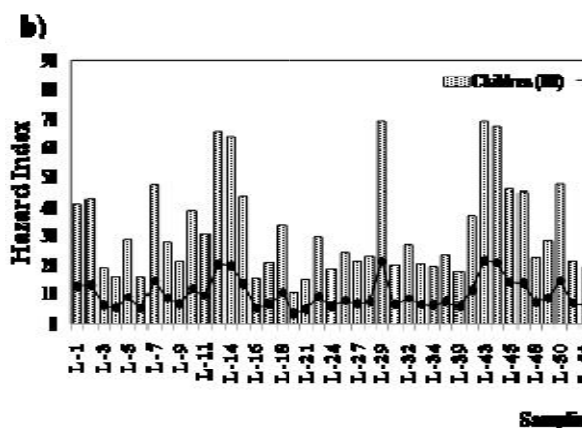


Figure 10. Health risk assessment As exposure through consumption of As contaminated drinking water in terms of hazard index (HI) among children, adult in a) monsoon and b) Post monsoon season

## 2.10 Speciation modelling of the groundwater for metal

In monsoon season total 13 minerals ( $\text{As}_2\text{O}_5$ , aragonite, brucite, calcite, dolomite(ordered), dolomite (disordered),  $\text{FeCO}_3$ , ferrihydrite (aged), fluorite, goethite, gypsum, mirabolite, NaF) were selected which are shown in the (Fig 20) for speciation modelling to confirm the possibility of solubility control for As and metal species. In this study observed that samples are super saturated with goethite,  $\text{FeCO}_3$  and ferrihydrite (aged) and some samples are in equilibrium state in ground water. Samples are also approaching almost equilibrium with calcite and gypsum. On other hand samples are under saturated with dolomite(ordered), dolomite (disordered), brucite, mirabolite, NaF, fluorite and  $\text{As}_2\text{O}_5$ ).

In post monsoon a total 14 minerals ( $\text{As}_2\text{O}_5$ , aragonite, brucite, calcite, dolomite (ordered), dolomite (disordered),  $\text{FeCO}_3$ , ferrihydrite (aged) fluorite, goethite, gypsum, halite, mirabolite, NaF) were selected shown in (Fig 21). Most of the samples are super saturated with goethite,  $\text{FeCO}_3$  and ferrihydrite. But three samples were approaching equilibrium for  $\text{FeCO}_3$  and in some sites calcite and gypsum are in almost equilibrium state. But as compared to monsoon calcite and gypsum are in less equilibrium state and samples are more spreads. Most of the samples are under saturated with calcite, dolomite (ordered), dolomite (disordered), brucite, halite, mirabolite, NaF, fluorite. In both season many minerals are in under saturated condition. So there will chance to increase the concentration of these minerals and

increase metal concentration in water.

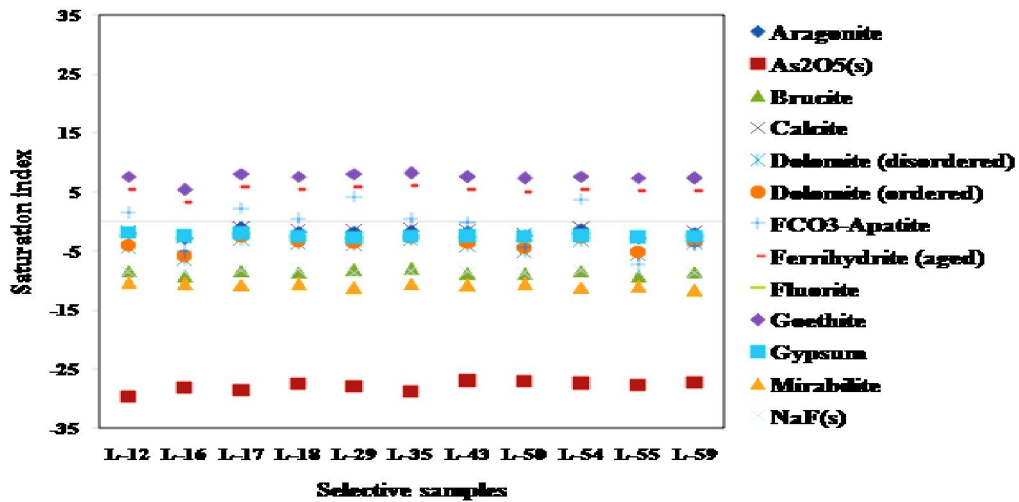


Figure 11 Saturation index of 13 minerals showing in monsoon for metal (n=11)

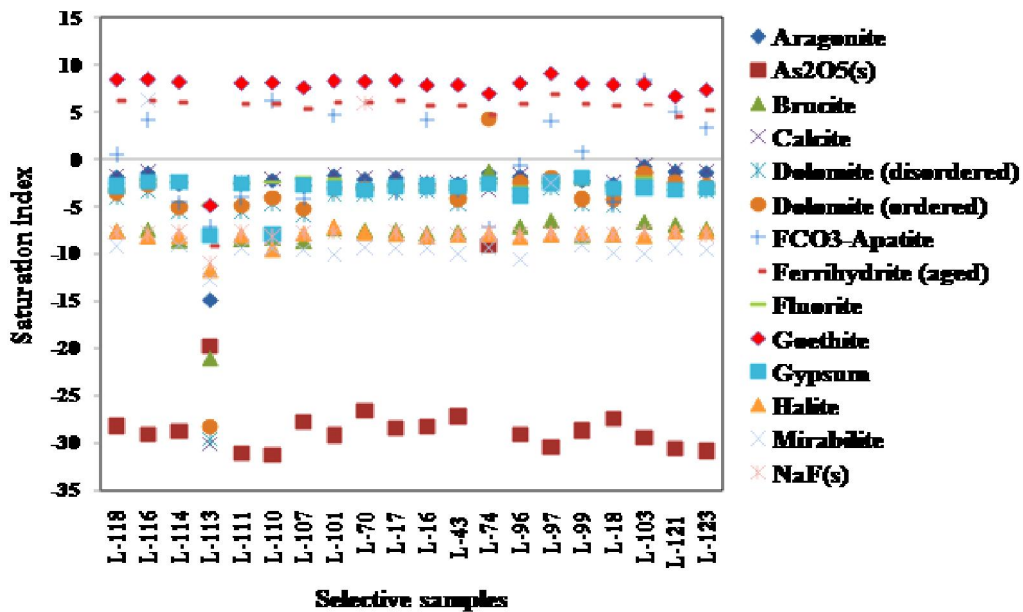


Figure 12 Saturation index of 14 minerals showing in post monsoon for meta l (n=20)

## 2.11 Sediment characterization

The sand content of all sediment cores was greater than silt and clay (Fig. 2a, b, Supplementary Table. 1) and changed little with season for samples S1-7. However,

for sediment samples D1-7, a marked increase in sand and a decrease in silt content was observed (**Fig. 2a, b**), while the sand percentage of samples R1-7 was greatly increased in the post-monsoon (**Fig. 2a, b**). This implies that the entire region consisting of the three rivers is highly prone to disturbance and channel migration, with the greatest disturbance due to annual flooding and sedimentation in the Ranganadi River (Goswami et al., 1999; Das et al., 2012; Borgohain et al., 2018). The intensity of flooding and the resultant disturbance can play a crucial role in As and F<sup>-</sup> mobilization to the groundwater as it brings a change in the particle composition which alters binding and release As and F<sup>-</sup>. There was notable variation in sediment pH from the monsoon to the post-monsoon season (**Fig. 2c, d**); during the monsoon the average pH was mainly neutral but became more alkaline toward the post-monsoon (**Fig. 2**). This phenomenon is the result of higher bicarbonate (HCO<sub>3</sub><sup>-</sup>) in the post-monsoon season arising from carbonate weathering (Kumar et al., 2016a).

The Fe and Mn content of the sediments (**Fig. 2e-h, Supplementary Table. 1**) were comparable for the Subansiri and Dikrong river plains. However, there was a decrease in the Ranganadi samples, which became more apparent during the post-monsoon season. Weathering and dissolution could be immediate but not very effective causes for the change, as Fe and Mn minerals are not easily soluble. The increase in sand content and resulting decline in overall surface area for Fe and Mn (hydr)oxides could be an important consideration (Xie et al., 2009). However, the change in the environmental condition to a more reducing state due to a sustained inundation by rains and annual floods at the beginning of the post-monsoon could also lead to the leaching of the Fe and Mn (hydr)oxides by reductive hydrolysis (Das et al., 2016). Calcium also showed a trend similar to Fe and Mn, as it dominated the Subansiri and Dikrong sediment samples compared to the Ranganadi samples (**Fig. 2i-j, Supplementary Table. 1**). The region under study is highly disturbed with a strong rainy season, floods, and periodic channel migration (Das et al., 2012; Borgohain et al., 2018), leading to much weathering and dissolution, and ultimately flushing of Ca<sup>2+</sup>, which could lead to lower cation exchange capacity of the sediments.

## 2.12 Arsenic fractionation

The sand and silt fraction contained the highest levels of physisorbed or most easily leached As, while clay had the highest levels of metal (hydr)oxide-bound and residual As (Lombi et al., 2000). Finer particles like silt and clay, having a higher surface area than sand, provide a larger binding area for metal (hydr)oxides, which in turn bind As (Appelo and Postma, 2005; Mohapatra et al., 2007). Fe and Al (hydr)oxides also form linkages with humic substances (Cheshire et al., 2000). Organic matter can greatly increase the groundwater As content especially in reducing aquifers with reducing bacteria (Guha et al., 2005; Wang and Mulligan, 2006). In this study, silt appears the most important particle fraction for holding As in the monsoon, as groundwater As was positively correlated with silt content (**Supplementary Table 2**). In the post-monsoon season, the percentage of sand and its correlation with groundwater arsenic increases manyfold (**Supplementary Table 2**). Both pH and anions like  $\text{HCO}_3^-$  can cause leaching of adsorbed As; alkaline pH may exceed the PZC of the Fe (hydr)oxides, while  $\text{HCO}_3^-$  and other anions can compete with As oxyanions for adsorption to positively charged sites on sediment particles (Smedley and Kinniburgh, 2002; Appel and Postma, 2005). Both the increase in the relative percentage of sand and elevation in pH result a net decrease in the total concentration of As in the sediments in the post-monsoon (**Fig. 3**). The percentage of clay was very low in the current study and did not show significant correlation with the various fractions of As extracted by the SEP (**Supplementary Table 2**).

Comparing **Fig. 3a, b and c**, the As in fraction I (physisorbed As) is very low compared to the others, except fraction IV in the post-monsoon season. Net As content in this fraction decreased from monsoon to the post-monsoon season. This was anticipated, as the physisorbed fraction is quite easily leached by other anions and the running water of the river. There was little variation in the distribution of this fraction among the three river floodplains; however, this fraction was depleted most in Ranganadi river sediments in the post-monsoon (**Fig 3b, c, Supplementary Table 3**). The prime reason is the highly disturbed nature of Ranganadi river, resulting in easier removal and flushing of this fraction, together with the deposition of an excess amount of sand.

Compared to a previous SEP study conducted on the BFP sediments (Kumar et al., 2016a), the current study reveals that fraction II constituted a significant percentage of the total As content (**Fig. 3b, c, Supplementary Table. 3**). The nature of its extraction by  $(\text{NH}_4)_2\text{HPO}_4$  (**Supplementary Fig. 1**) suggests that this fraction will be significantly impacted by the addition of agricultural phosphates like triple super phosphate  $[\text{Ca}(\text{H}_2\text{PO}_4)_2\text{H}_2\text{O}]$  and glyphosate ( $\text{C}_3\text{H}_8\text{NO}_5\text{P}$ ), both known to contain arsenic as an impurity (Jayasumana et al., 2015). We observed a decrease in the As level from monsoon to the post-monsoon season (**Fig. 3b, c, Supplementary Table 3**) in the sediments of rivers Subansiri and Dikrong (**Fig. 3b, c, Supplementary Table 3**). The most probable reason appears to be interference by agricultural runoff containing agrochemicals, as most of the sampling points had agricultural fields in close proximity.

The Fe (hydr)oxide-associated As in the sediment samples are represented by fractions III (amorphous and poorly crystallized) and IV (well crystallized). Fraction IV is quite low in all sediment samples irrespective of the river, it diminished to negligible levels by the post-monsoon (**Fig 3 and Supplementary Table 3**). This suggests amorphous and poorly crystallized Fe (hydr)oxides like ferrihydrite, along with fraction II, comprise the dominant As pools with groundwater contamination potential. Toward the post-monsoon there is a change to a more anoxic state because of the submerged conditions. This reducing environment leads to the depletion of not only fraction IV to negligible levels, but fraction III also undergoes reductive dissolution, contributing to its depletion (**Fig. 3 and Supplementary Table 3**).

Residual As extracted by  $\text{HNO}_3 + \text{H}_2\text{O}_2$  is generally associated with minerals like sulphides and with organic matter (Wenzel et al., 2001; Mihaljevič et al., 2003), and is very difficult to remove under normal conditions. It is the least likely to contribute to the As content of the groundwater in the sampled areas. Comparison of monsoon and the post-monsoon sediments shows a difference in this fraction. Depletion of residual As (**Supplementary Table. 3**) was observed in some of the samples (**R2 to R7**). Residual As may be greater in finer particles like silt. Since sand becomes dominant at the expense of silt in the Ranganadi sediments (**Supplementary Table. 1**), there is an observed depletion in residual As during the post-monsoon season.

### 2.13 Partition coefficient as a tool to understand “specific mobility”

The partition coefficients ( $K_d$ ) of the different arsenic fractions help in understanding their contribution to specific mobility and groundwater contamination. During the monsoon season,  $K_{d1}$  was negatively correlated ( $r=-0.54$ ) with fraction II, while  $K_{d2}$  had a positive correlation ( $r=0.56$ ) with fraction III (**Supplementary Table 2**). As the sum of fractions I+II was considered to be arsenic in solution ( $C_L$ ) for calculating  $K_{d1}$ , a significant increase in either fraction will decrease  $K_{d1}$ , assuming As remained constant in the other fractions (Kumar et al., 2016a). An increasing level of As associated with fraction II will decrease  $K_{d1}$  and this fraction was positively correlated ( $r=0.69$ ) with groundwater As (**Supplementary Table 2**). Thus compared to fraction I, fraction II (chemisorbed As) has a much more significant contribution to the groundwater As level, mainly because of the greater amount of As associated with this fraction. Groundwater As also had highly positive correlations with fractions III and IV ( $r=0.92$  and  $0.89$ , respectively), signifying Fe (hydr)oxides as the primary source of As (**Supplementary Table. 2**). Thus, any increase in these two fractions will be directly reflected in elevated groundwater As. This also explains why  $K_{d2}$  has a positive correlation with fraction III, as total As in the sediments is a summation of the five fractions. Any increase in contribution of fractions III and IV would mean an increase in  $K_{d2}$  or a positive correlation. An important finding was the non-observance of any correlation between  $K_{d1}$  and  $K_{d2}$ , which could be due to the dependence of  $K_{d1}$  primarily on fraction II, while  $K_{d2}$  is influenced mainly by fraction III.

In the post-monsoon season, As extracted from fractions I and II decreases due to geogenic leaching during the monsoon season (**Supplementary Table 3**). Therefore, the importance of these fractions is diminished in terms of total contribution to groundwater As. This is supported by the absence of significant correlations of fraction I or II with  $K_{d1}$  (**Supplementary Table 2**); however, groundwater As levels still correlated positively with fraction II ( $r=0.6$ ). At the same time,  $K_{d2}$  showed a negative correlation ( $r=-0.52$ ) with fraction I, indicating its smaller contribution to groundwater As. A positive correlation between  $K_{d1}$  and  $K_{d2}$  in the post-monsoon indicates a larger contribution of fractions other than physisorbed and chemisorbed phases, since  $K_{d1}$  is dependent on fraction I and II. This was determined to be amorphous Fe (hydr)oxides, which acted as the principal source of As in groundwater. This is supported by the

stronger positive correlation of fraction III with groundwater As and  $K_{d1}$  ( $r=0.71$  and  $0.63$  respectively, **SupplementaryTable. 2**), and a moderate correlation with  $K_{d2}$  ( $r=0.46$ , **Supplementary Table 2**). Any significant contribution due to fraction I or II will be expressed as a negative correlation with  $K_{d1}$ , as  $C_L$  is calculated as their sum, assuming the other fractions remain constant. Fraction V was also positively correlated with groundwater As and  $K_{d1}$  ( $r=0.65$  and  $0.54$  respectively, **SupplementaryTable 2**). As fraction V is the residual As, the correlations likely arise because of the overall higher levels of As associated with this fraction, irrespective of the mobility.

#### 2.14 Batch desorption experiment

The importance of the Fe (hydr)oxides fraction was assessed prior to the batch desorption by the SEP and extraction of total Fe from the sediment samples. Significant Fe was extracted from sediment samples in both monsoon and post-monsoon seasons (**Fig. 2e, f**). The involvement of reductive hydrolysis is suggested by the decline in Fe content from monsoon to post-monsoon, as discussed previously. At the same time, Mn (hydr)oxides are not likely a major reservoir of As, as Mn extracted from the sediments was far less than Fe (**Fig. 2g, h, Supplementary Table 1**). The importance of the (hydr)oxide fraction is also revealed by the high positive correlation between Fe and Mn during both monsoon and post-monsoon seasons ( $r = 0.79$  and  $0.9$ , **SupplementaryTable 2**). This could be due to the presence of the major load of these trace elements in the (hydr)oxides phases, which form coatings on sediment particles.

Removal of Fe (hydr)oxides resulted in a difference in the quantity of As leached (**Fig. 4**). Raw samples in both monsoon and post-monsoon leached far more As at all three pH levels compared to the CBD-treated samples (**Fig. 4**). A higher amount of Fe (hydr)oxides results in adsorption of greater quantities of As which could be leached under alkaline pH, resulting in the trend observed (Goldberg and Johnston, 2001; Kim et al., 2012; Kumar et al., 2016a). For raw samples, during the monsoon season, Ranganadi sediments showed the highest desorption among the three river sediments at acidic, neutral and alkaline pH. This is because Ranganadi sediments had the highest amount of Fe (hydr)oxide-associated As compared to the other sediments (**Fig. 4a, Supplementary Table 3**). In the post-monsoon season, we observed less As desorption

for Subansiri and Ranganadi sediments compared to the monsoon values (**Fig. 4b, Supplementary Table. 4**). It is especially low for Ranganadi, which had the highest As desorption in the monsoon season. Conversely, As desorption increased in the sediments of the Dikrong river (**Fig. 4b**). This can be attributed to speciation of As based on the change in environmental conditions brought about by the changing season.

The relationship between average total As in the Fe (hydr)oxides (Fraction III+IV) from the three sediment groups and the average leached quantity at pH 7 and 10 was strongly positive in the monsoon season (**Fig. 5a and b, respectively**). This supports the prevalence of arsenate, leading to desorption-based leaching at higher pH. We did not observe any positive relationship between the average leached As at pH 7 and 10 and average As extracted from fractions III+IV in the three sediment groups in the post-monsoon season (**Fig. 5c and d respectively**). This suggests that water-saturated conditions created a more anoxic condition, leading to a larger percentage of arsenite during the post-monsoon season compared to the monsoon season. Even loosely bound arsenite in the pore water could become strongly adsorbed at highly alkaline pH. Submerged sediments appear more pronounced in the river Ranganadi in the post-monsoon, resulting in much less desorption than in the monsoon (**Fig. 4b**). This may be attributed to the fact that arsenite is known to have a sorption maximum between pH 7 to 8.5 or even higher compared to pH 4 for arsenate (Masscheleyn et al., 1991; Goldberg and Johnston, 2001). Therefore, despite the PZCs of Fe (hydr)oxides being in the range of 8.5 to 9.3 (Kim et al., 2012), the comparatively similar sorption maxima of arsenite results in less desorption in the post-monsoon season.

Desorption from the CBD-treated sediments showed marked departure from that of the raw sediments (**Fig. 4c, d**). The As remaining after CBD treatment is negative for Dikrong and Ranganadi sediments in monsoon and post-monsoon seasons, respectively (**Supplementary Table 4**). The amount of Fe (hydr)oxide associated As remaining after treatment in the Ranganadi sediments during the monsoon season is significantly higher than in the other sediments. This resulted in greater desorption at higher pH (pH 7 and 10, **Fig. 4. c, d and, 5**) than for the other two sediment groups where the Fe (hydr)oxide removal was much more efficient, resulting in significantly lesser adsorption during spiking (**Supplementary Table 4**). As a result, the desorption pattern for Ranganadi sediments during the post-monsoon mimicked the monsoon

season. At pH 5, arsenate oxyanions are more strongly bound to the Fe (hydr)oxides, resulting in less leaching from the Ranganadi samples compared to the other samples (**Fig. 4c, d**), as observed from the negative correlation between the amount of As leached and that remaining after CBD treatment at pH 5 (**Fig. 5**).

### 2.15 “Operationally defined fractions” of fluoride

F<sup>-</sup> was positively correlated with Fe extracted from all the sediments (**Fig. 6a**) during both monsoon and post-monsoon seasons. Fluoride was also weakly correlated with Mn (**Fig. 6b**), but the quantity of Mn extracted from the sediments was much lower than Fe, implying that Fe (hydr)oxides are the dominant secondary reservoir of F<sup>-</sup> compared to Mn (hydr)oxides. The primary source of F<sup>-</sup> in the groundwater of the region, however, appears to be F<sup>-</sup> bearing minerals like fluorite (NaF), calcite (CaF<sub>2</sub>) and fluorapatite (Ca<sub>5</sub>(PO<sub>4</sub>)<sub>3</sub>F), supported by the positive relationship between F<sup>-</sup> extracted from the sediments and their Na and Ca contents (**Fig. 6c, d**). The environmental conditions working to mobilize As were not favorable for F<sup>-</sup> leaching, as no relationship between F<sup>-</sup> and the total As extracted from the sediments was observed (**Fig. 6f, Supplementary Table 5**). Re-adsorption of F<sup>-</sup> on many of the freed adsorption sites after the subsidence of the monsoon and flood season could explain this observation. The F<sup>-</sup> content of fractions III and IV is prominent (**Supplementary Table 5**), indicating that reductive dissolution is resulting in the release and depletion of F<sup>-</sup> in the Fe (hydr)oxides fractions, followed by re-precipitation of F<sup>-</sup> during the calmer post-monsoon season. Overall, two major observations are that the secondary reservoirs of F<sup>-</sup> did not appear limited to Fe (hydr)oxides but included the other fractions as well and the total content of a contaminant in the sediment may not be a good indicator of its actual contamination potential.

### 2.16 Co-occurrence and Co-leaching perspective of As and F

Previous research has documented co-occurrence of As and F<sup>-</sup> in groundwater under different environmental conditions across the world (**Table 1**). Careful observation reveals that most of the regions with high concentrations as well as strong

positive correlations between groundwater As and F<sup>-</sup> experience arid oxidizing conditions (Nicolli et al., 1989; Warren et al., 2005; Gomez et al., 2009; Brahman et al., 2013a; Rasool et al., 2015). Such co-occurrence is mainly due to desorptive co-release of As and F<sup>-</sup> from Fe (hydr)oxides; however, other probable causes like dissolution of arsenic rich volcanic glass accompanied by calcite dissolution (Nicolli et al., 1989; Gomez et al., 2009) have also been documented. Thus, in arid environments, the relationship between As and F<sup>-</sup> becomes much more apparent as the As load mainly exists as As(V) displaying sorption behavior similar to F<sup>-</sup> or due to the abundance of minerals like volcanic glass in special cases not found in humid alluvial plains. Sequential extraction and batch desorption has helped advance this knowledge, especially in regions such as alluvial plains where the relationship between the two contaminants is not very clear (Kumar et al., 2016b). As F<sup>-</sup> requires a very stable dry groundwater environment for enrichment, co-occurrence is very difficult to observe, especially in humid alluvial plains like the BFP. However, simulating different leaching scenarios in the laboratory can be useful, as exemplified by Kim et al. (2012). As the BFP is also a humid flood plain with conditions unsuitable for F<sup>-</sup> enrichment in close proximity to the river (Das et al., 2016), SEPs and batch desorption were conducted to study probabilistic scenarios of As and F<sup>-</sup> co-occurrence (Kumar et al (2016b). This revealed that isolated drier aquifers at greater distance from the river could be common ground for F<sup>-</sup> and As enriched groundwater. In the current study we expanded this approach to other regions of the BFP which have remained unexplored via SEP and desorption simulation.

## **2.17 Biochar characterization**

### **2.17.1 Proximate and elemental analysis**

The proximate and elemental analysis of activated biochar and biochar at different temperatures for *S. ravannae* sample are summarized in Table 1.

Table 1: Physicochemical properties of *S. ravannae* biochar at different temperatures and activated biochar

Properties	Biochar					Activated biochar
	350°C	400°C	450°C	500°C	550°C	
pH	9.44±0.02	9.51±0.02	9.58±0.07	9.66±0.05	9.81±0.03	12.01±0.20
EC (m mho cm <sup>-1</sup> )	0.16±0.01	0.24±0.01	0.31±0.01	0.45±0.02	0.79±0.01	1.11±0.02
Water content	6.49±0.01	5.88±0.03	5.21±0.01	4.94±0.02	4.5±0.02	1.48 ± 0.05
Volatile matter	39.62±0.24	35.46±0.18	32.68±0.15	30.93±0.24	26.35±0.30	15.8 ± 0.32
Ash content	6.96±0.02	7.15±0.08	8.53±0.10	8.93±0.06	9.11±0.10	2.18 ± 0.07
Fixed carbon	46.93±0.49	51.51±0.22	53.58±0.15	55.19±0.38	60.04±0.32	80.54±0.25
C	56.71	58.95	60.97	62.27	63.81	73.42
H	3.04	2.86	2.57	2.48	2.14	2.05
N	2.82	2.51	2.32	1.53	1.62	1.59
O <sup>a</sup>	37.43	35.68	34.14	33.72	32.43	22.94
H/C	0.6391	0.578	0.503	0.475	0.4	0.33
O/C	0.496	0.455	0.421	0.407	0.382	0.23
BET surface area (m <sup>2</sup> /g)	5.57	50.6	201.5	237.2	319.2	1248.2

*S. ravannae* has a very high volatile matter content which reduces drastically after pyrolysis. It indicates higher conversion of biomass to liquid and gaseous products (Morali et al. 2015). As a result of decrease in volatile matter content, fixed carbon of the biochar increased significantly which means there is less liberation of fixed carbon. Because of the further carbonization at higher temperature, the ratios of all elements except carbon significantly decreased for activated carbon. It was observed that with increase in pyrolysis temperature, H/C and O/C ratios of the biochars decreased. This may be due to the fact that oxygen containing functionalities are decomposed by decarbonylation and decarboxylation followed by transformation to the alkyl-aryl C—C bonds as a cross-linking between small aromatic rings (Mullen et al. 2015). Also, for activated biochar, significant drop in H/C and O/C ratios indicates the rise of aromaticity and hydrophobicity and the reduction of polar groups (Tan et al. 2016). It was observed from Table 1 that with increase in pyrolysis temperature, the pH values of the biochar and activated biochar increased, as at higher pyrolysis temperatures concentration of alkali salts increases due to removal of organic materials from biochar.

### 2.17.2 Electrical conductivity (EC)

The EC values of the *S. ravannae* biochars were found to increase with increase in pyrolysis temperatures. Also, activated biochar has higher value of EC than raw biochar. Soil containing biochar having higher EC value may harm plant growth by reducing water uptake and cause nutrient imbalance due to increased salinity (Bordoloi et al. 2015).

### 2.17.3 Fourier Transform Infra-red Spectroscopy (FTIR)

FTIR spectras for activated biochar and biochar at optimum condition are presented in supplementary document S3. The peak around  $3413\text{ cm}^{-1}$  for biochar corresponding to O–H stretching vibration, was strengthened after activation (Tan et al. 2015; Bordoloi et al. 2016). Peaks appeared at around  $2924\text{ cm}^{-1}$  are attributed to the C–H stretching vibration of alkanes from CH and CH<sub>2</sub> in cellulose and hemicellulose components. The presence of carbonyl group in the biochar is limited as observed in the region  $1650\text{--}1750\text{ cm}^{-1}$  and was significantly weakened for the activated carbon. The peaks appeared at around  $1591\text{ cm}^{-1}$  provides the evidence of C=C bond of alkene and aromatics present in the biochar which disappeared for activated carbon due to its highest degree of carbonization and the lowest oxygen ratio. The band observed in the region  $1340\text{--}1480\text{ cm}^{-1}$  indicate the presence of phenol (Gautam et al. 2015). The bands at around  $1079\text{ cm}^{-1}$  and  $750\text{ cm}^{-1}$  were due to C–O stretching vibration of polysaccharides and aromatic –CH scissoring respectively which were found to be slightly changed after activation. The observed functional groups have been reported as chemical groups for characterization of many other carbon based sorbents including biochar and activated carbon (Chenet et al. 2014). The obtained results demonstrated the difference in the type and concentration of surface functional groups which may affect the capacity and mechanism for the removal of pollutants.

### 2.17.4 Raman spectroscopy

The defects and crystallization degree of activated biochars were estimated by Raman spectroscopy (supplementary document S4). The nomenclature for Raman bands had been followed as per Mohanty *et al.*, 2013. The band at  $1174\text{ cm}^{-1}$  (S band) and  $1228\text{ cm}^{-1}$  (S<sub>L</sub>) indicated the strong intensity for aryl-alkyl ether

bonding. The 1000–1250  $\text{cm}^{-1}$  region is referred to as the multiple bond  $\gamma$  (C=S). The 600–1300  $\text{cm}^{-1}$  region is referred as a strong intensity region for alicyclics and aliphatic chains of  $\gamma$  (C=C) as found in activated biochars. The bands between 1366  $\text{cm}^{-1}$  (D band) and 1461  $\text{cm}^{-1}$  ( $V_L$ ) indicated methylene or methyl groups. Significant bands at 1540  $\text{cm}^{-1}$  ( $G_R$  band) to 1703  $\text{cm}^{-1}$  ( $G_L$  band) were from aromatic compounds, whereas the band specific to 1616  $\text{cm}^{-1}$  (G band) is referred to  $\gamma$  (C=C) aromatic groups or alkene C=C vibrations. Other two bands such as 1568 and 1634  $\text{cm}^{-1}$  indicated  $\gamma$  (N=N) aliphatic substitutes and  $\gamma$  (C=N) structures, respectively. The D band represented higher aromatic rings ( $\leq 6$  fused rings), while  $G_R$ ,  $G_L$  and  $V_L$  represented the amorphous components with smaller fused aromatic rings. The S and  $S_L$  bands were due to the presence of H structures in monomeric form. In the samples, the  $V_L$  band represented the amorphous carbon structures. The S band, assigned to  $sp^2$ – $sp^3$  carbeneous structures, gives similar information to that of the crystallinity measurement through XRD analysis.

### 2.17.5 Scanning electron microscopy (SEM)

The porous structure of the biochar and activated biochar can be clearly seen in the SEM images obtained at optimum experimental conditions by CCD (supplementary document S5). The porous structure and the holes on the surface of the *S. ravannae* biochar, created during pyrolysis, provided more adsorption sites for ions, space for nutrients and water retention (Morali et al. 2015). These pores were more prominent in activated biochars as observed from supplementary document S5. It suggested that the biochar after chemical activation produced a large number of pores which greatly increased the specific surface area following the improved adsorption uptake of the material. This was consistent with the findings from BET analysis for surface area measurement.

### 2.17.6 Brunauer–Emmett–Teller (BET) analysis

Surface area is one of the main factors that control a matter's potential to adsorb chemical compounds, as the total pore volume and surface area of solid fuels affect the combustion characteristics of bio-chars as fuels. BET surface area of 5.57  $\text{m}^2 \text{g}^{-1}$  was measured for the biochar obtained at 350°C which is very low in comparison to typical

activated carbon. Thus, the biochar obtained from *S. ravannae* is not appropriate for direct usage as activated carbon application. However, BET surface area of 1248.2 m<sup>2</sup> g<sup>-1</sup> of the activated biochar demonstrates its potential use as a support material for solid catalyst (Sut et al. 2016).

#### **2.17.7 X-ray diffraction spectroscopy**

X-ray diffraction is considered as a widely applicable technique for analysing the crystallinity of biomass and biochar structure. No significant changes were observed for the biochar and activated biochar in their XRD spectras. Similar results were also found for biochar and activated biochar for corn straw by Tan *et al.* 2016 (Tan et al. 2016). The XRD spectra (Supplementary document S6) showed a broad peak at the 2θ values of around 20–30. This peak indicated the development of increasingly carbonized material and provided evidence for presence of a graphitic structure in the biochar samples (Chutia et al. 2014). This peak comes from the formation and successive ordering of aromatic carbon in the biochar and modified biochar samples. The presence of a higher amount of aromatic compound in the samples as evidenced from FTIR spectra was further supported by the XRD pattern.

#### **2.17.8 EDX**

From the EDX analysis (supplementary figure S7) of activated biochar before and after adsorption, it was observed that the activated biochar from *S. ravannae* primarily consists of various inorganic elements important for soil fertility and crop production (Chutia et al. 2014). Further, comparison of EDX images shows no significant variations of element composition for before and after incorporation of As and F<sup>-</sup> ions.

#### **2.17.9 Central composite design (CCD) and statistical analysis**

The complete design matrix of the experiments and the response for As and F<sup>-</sup> adsorption are presented in Tables 2 and 3 respectively.

Removal efficiency ( $A_s$ ) =

$$90.20 - (0.95 \times \text{initial concentration}) - (0.37 \times \text{contact time}) + (532.23 \times \text{adsorbent dose}) + (1.96 \times \text{initial concentration} \times \text{contact time}) - (3.09 \times \text{initial concentration} \times \text{adsorbent dose}) + (1.91 \times \text{contact time} \times \text{adsorbent dose}) + (6.01 \times \text{concentration}^2) + (5.99 \times \text{contact time}^2) + (0.31 \times \text{adsorbent dose}^2) \quad (11)$$

Removal efficiency ( $F$ ) =

$$39.86 - (3.1 \times \text{initial concentration}) - (9.26 \times \text{adsorbent dose}) + (0.27 \times \text{contact time}) - (0.88 \times \text{initial concentration} \times \text{adsorbent dose}) + (0.22 \times \text{initial concentration} \times \text{contact time}) - (3 \times \text{adsorbent dose} \times \text{contact time}) + 0.05 \times \text{concentration}^2 + (269.63 \times \text{adsorbent dose}^2) + (2.70 \times \text{contact time}^2) \quad (12)$$

where initial concentration is in  $\text{mg L}^{-1}$ , contact time is in minute and adsorbent dose is in g per 50 mL.

**Table 2: Experimental design matrix and results for arsenic adsorption**

Std.	Run	Actual level of factors			Coded level of factors			Removal efficiency (%)
		Initial concentration (mg/L)	Contact time (minute)	Adsorbent dose (g/50 ml)	A	B	C	
1	1	100	20	0.02	1	-1	-1	67.1
2	2	65	40	0.035	0	0	0	69.4
3	3	65	40	0.035	0	0	0	69.4
4	4	65	40	0.035	0	0	0	69.4
5	5	30	60	0.02	-1	1	-1	82.6
6	6	123.863	40	0.035	1.682	0	0	70.5
7	7	65	40	0.060227	0	0	1.682	78.6
8	8	65	40	0.035	0	0	0	69.4
9	9	65	40	0.009773	0	0	-1.682	51.5
10	10	30	20	0.02	-1	-1	-1	77.5
11	11	65	40	0.035	0	0	0	69.4
12	12	30	20	0.05	-1	-1	1	95.5
13	13	65	73.6359	0.035	0	1.682	0	86.5
14	14	65	6.36414	0.035	0	-1.682	0	55.4
15	15	6.13725	40	0.035	-1.682	0	0	99.5
16	16	65	40	0.035	0	0	0	69.4

17	17	100	60	0.05	1	1	1	88.5
18	18	100	60	0.02	1	1	-1	74.7
19	19	30	60	0.05	-1	1	1	99.9
20	20	100	20	0.05	1	-1	1	75.6

The experimental results obtained for removal efficiency (%) of As and F<sup>-</sup> were fitted to second degree polynomial model, which can be represented by Eqs.11 and 12 respectively in terms of actual factors.

The interaction between the independent variables as well as significance of each model term were established by analysis of variance (ANOVA) and the results obtained are presented in Tables 4 and 5 for As and F<sup>-</sup> respectively.

**Table 3: Experimental design matrix and results for fluoride adsorption**

Std.	Run	Actual level of factors			Coded level of factors			Removal Efficiency (%)
		Initial concentration (mg/L)	Contact time (minute)	Adsorbent dose (g/50 ml)	A	B	C	
1	1	25	0.5	60	1	1	1	18.5
2	2	4.88655	0.35	40	-1.682	0	0	35.2
3	3	17.5	0.35	6.36414	0	0	-1.682	21.5
4	4	17.5	0.35	40	0	0	0	9.6
5	5	10	0.5	20	-1	1	-1	50
6	6	25	0.5	20	1	1	-1	40
7	7	17.5	0.097731	40	0	-1.682	0	17.5
8	8	10	0.2	20	-1	-1	-1	21.5
9	9	25	0.2	60	1	-1	1	30
10	10	17.5	0.602269	40	0	1.682	0	43.3
11	11	17.5	0.35	40	0	0	0	21.5
12	12	10	0.5	60	-1	1	1	21.5
13	13	17.5	0.35	40	0	0	0	7.5
14	14	17.5	0.35	40	0	0	0	21.9
15	15	17.5	0.35	40	0	0	0	8.7
16	16	30.1134	0.35	40	1.682	0	0	9.7
17	17	25	0.2	20	1	-1	-1	9.2
18	18	10	0.2	60	-1	-1	1	22.7

19	19	17.5	0.35	73.6359	0	0	1.682	11.1
20	20	17.5	0.35	40	0	0	0	21.5

Significance of each term can be determined by using both F-value and Prob >F values. The larger F-value indicate that the term is significant. Model F-value of 8.53 for As adsorption and 6.42 for F<sup>-</sup> adsorption implies a significant model. There is only a 0.12% chance that for the model 'F-value', this large could occur due to noise (Tables 4 and 5). Values of 'Prob >F' lower than 0.05 indicate that the model terms are significant while values greater than 0.1 indicate the model terms are not significant. In the case of As adsorption, the significant model terms are initial concentration, contact time, adsorbent dose and square of initial contraction having F-value 19.1, 13.37, 21.01 and 21.05 respectively (Table 4).

**Table 4: ANOVA for response surface quadratic model for arsenic removal**

Source	Sum of		Mean	F	P-value	
	Squares	df	Square	Value	Prob > F	
Model	2849.1	9	316.57	8.53	0.0012	significant
A-concentration	708.59	1	708.59	19.1	0.0014	
B-time	496.01	1	496.01	13.37	0.0044	
C-dose	779.49	1	779.49	21.01	0.001	
AB	15.13	1	15.13	0.41	0.5375	
AC	21.13	1	21.13	0.57	0.4679	
BC	2.64	1	2.64	0.071	0.7949	
A <sup>2</sup>	781.03	1	781.03	21.05	0.001	
B <sup>2</sup>	82.62	1	82.62	2.23	0.1665	
C <sup>2</sup>	1.37	1	1.37	0.037	0.8514	
Residual	370.96	10	37.1			
Lack of Fit	370.96	5	74.19			
Pure Error	0	5	0			
Cor Total	3220.06	19				

**Table 5: ANOVA for response surface quadratic model for fluoride removal**

Source	Sum of Squares	df	Mean Square	F Value	p-value Prob > F	
Model	2394.18	9	266.02	6.42	0.0038	significant
A- concentration	271.44	1	271.44	6.55	0.0284	
B-dose	592.98	1	592.98	14.3	0.0036	
C-time	151.53	1	151.53	3.66	0.0849	
AB	8	1	8	0.19	0.6698	
AC	88.45	1	88.45	2.13	0.1748	
BC	648	1	648	15.63	0.0027	
A <sup>2</sup>	152.79	1	152.79	3.69	0.0838	
B <sup>2</sup>	530.44	1	530.44	12.8	0.005	
C <sup>2</sup>	16.86	1	16.86	0.41	0.5379	
Residual	414.56	10	41.46			
Lack of Fit	157.43	5	31.49	0.61	0.6983	not significant
Pure Error	257.13	5	51.43			
Cor Total	2808.73	19				

In case of  $F^-$  adsorption, significant model terms are initial concentration, adsorbent dose, interaction term between adsorbent dose and contact time and square term for adsorbent dose having F-value 6.55, 14.3, 15.63 and 12.8 respectively (Table 5). The coefficient of determination,  $R^2$  for the As adsorption model and  $F^-$  adsorption model is 0.8848 (Table 4) and 0.8524 (Table 5) respectively. Again, adjusted  $R^2$  improves  $R^2$  in relation to the sample size and the model terms and the corresponding values for As and  $F^-$  adsorption are 0.7811 and 0.7196 respectively. Both the  $R^2$  and adjusted  $R^2$  values for the model is high enough and comparable signifying that the selected model satisfactorily defines the experimental data within the selected operating conditions. Adequate precision (Adeq Precision) measures the signal to noise ratio and a ratio more than 4 is desired. In the present study, the value of Adeq Precision for As and  $F^-$

adsorption are 10.395 and 10.267 respectively indicating adequate signal and the model can be used to navigate the design space.

### 2.17.10 Model validation and response surface plot

The adequacy of the model was established by using diagnostic plot (normal % probability versus studentized residuals and studentized residuals versus run number) which are presented in Figs.1a-b and Figs.2a-b for As and F<sup>-</sup> adsorption respectively.

For both the cases, in Fig.1a and Fig.2a, the points are spread almost on a straight line along the diagonal. This trend shows that the error terms are normally dispersed and independent of each other. Also, it was observed in Fig.1b and Fig.2b that the points are randomly scattered surrounding zero on the studentized residuals axis in between +4.5 and – 4.5 in both the cases, which indicates homoscedasticity and establishing the adequacy of the respective model for.

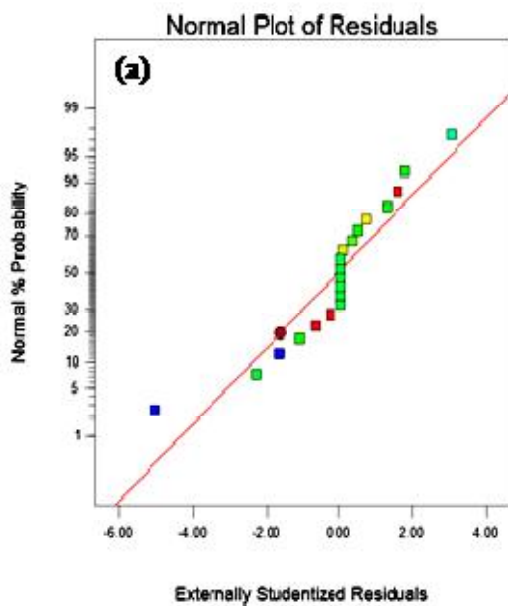


**Figure 1:** Diagnostic plot the model for arsenic (a) Normal % probability versus studentized residuals, (b) Studentized residuals versus run number

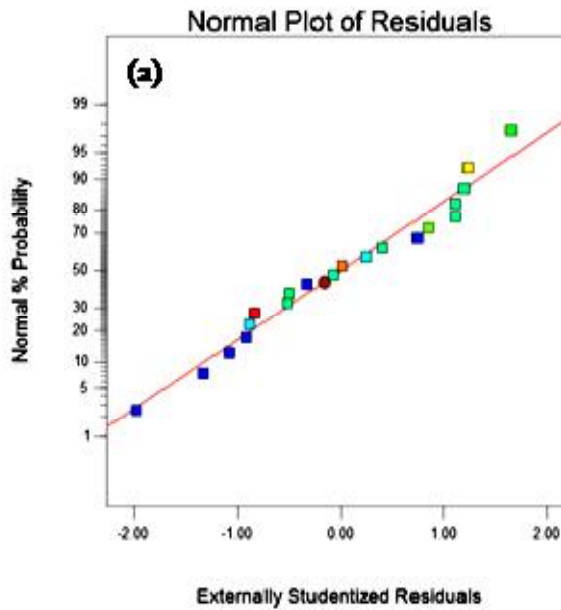


**Figure 2: Diagnostic plot the model for fluoride (a) Normal % probability versus studentized residuals, (b) Studentized residuals versus run number**

### 2.17.11 Effect of initial concentration

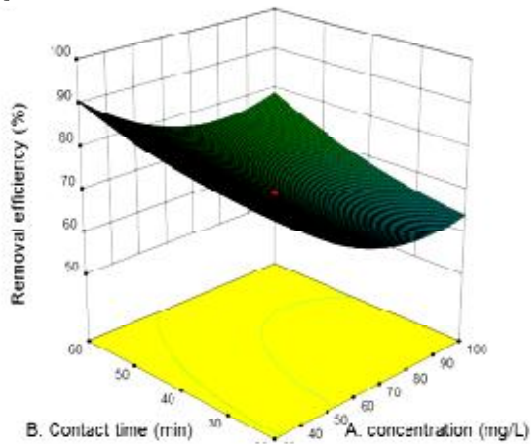
Three-dimensional (3D) surface plots were used to study the concurrent effect of independent variables on the removal efficiency which are presented in Figs.3a-f and Figs.4a-f for As and F<sup>-</sup> adsorption respectively.

For As removal, Fig.3a and Fig.3c show the combined effect of initial concentration with contact time and adsorbent dose respectively. It is clear from Fig.3a and Fig.3c that percentage removal decreases gradually with increasing initial concentration. At low concentration, enough adsorption site onto activated biochar surface existed for adsorption and vice-versa. Hence, with increase in initial concentration, adsorption was found to be decreased (Massoudinejad et al. 2016). Contour plots of initial concentration vs contact time (Fig.3b) and initial concentration vs adsorbent dose (Fig.3d) indicate similar results with 3D surface plot. For F<sup>-</sup> removal, the collective effect of initial concentration with contact time and adsorbent dose are presented in Fig.4a and Fig.4c respectively. The Fig. 4a and Fig.4c depicts that with increase in F<sup>-</sup> concentration, percent removal decreased gradually. The contour plots in Fig. 4b and Fig. 4d indicate similar results for F<sup>-</sup> adsorption.

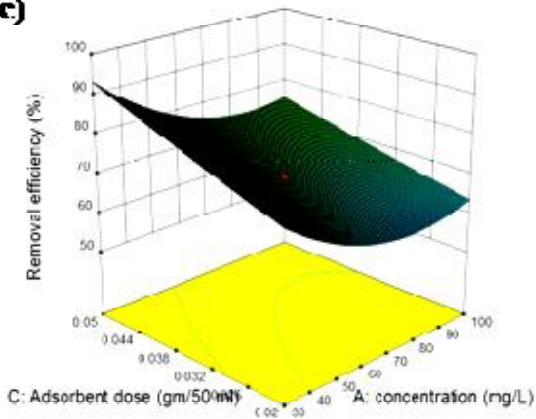
### **2.17.12 Effect of adsorbent dose**

The combined effect of adsorbent dose with initial concentration and contact time for As removal are presented in Fig. 3c and Fig. 3e respectively. It is observed from both the figures that removal efficiency increases with increase in adsorbent dose. Similar result for the collective influence of adsorbent dose with initial concentration and contact time for F<sup>-</sup> removal are observed in Figs. 4c and 4e respectively. An increase in adsorption with adsorbent dosage can be attributed to a greater surface area and the availability of more adsorption sites at higher adsorption dosage (Mourabet et al. 2015). The contour plots in Figs. 3d and 3f for As removal and Figs. 4d and 4f for F<sup>-</sup> removal indicate similar results as described in 3D graphs.

(a)



(c)



(e)

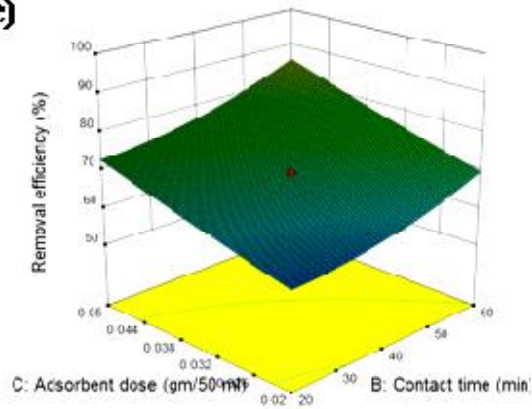


**Fig.3: Interaction graphs and the corresponding surface response plots for the combined effects of process variables on removal efficiency. (a) and (b) effect of initial Arsenic concentration and contact time; (c) and (d) effect of arsenic initial concentration and adsorbent dose at constant contact time; (e) and (f) effect contact time and adsorbent dose at constant Arsenic initial concentration.**

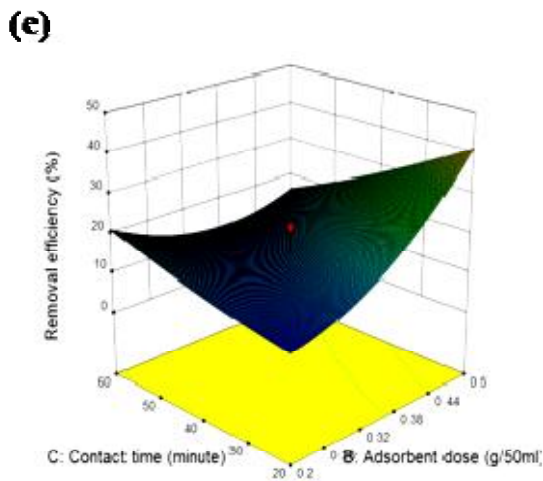
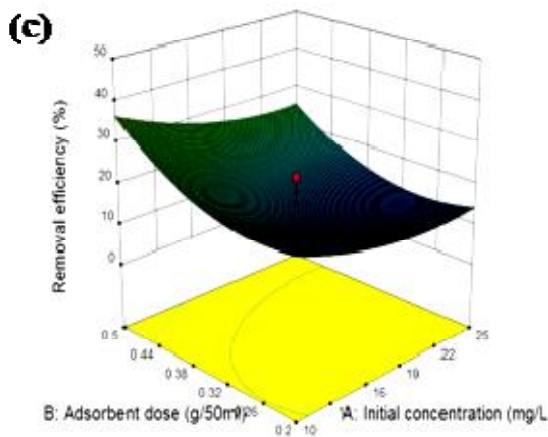
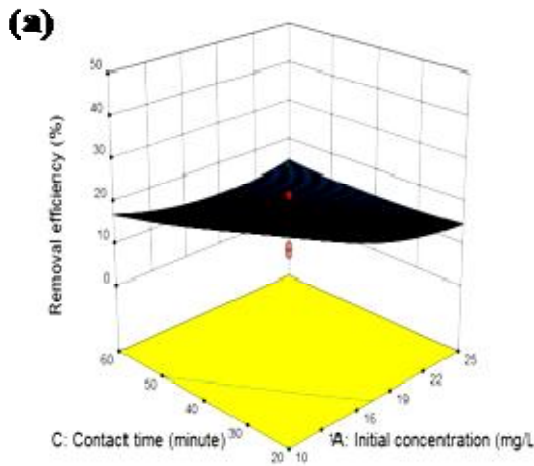


**Fig.4:** Interaction graphs and the corresponding surface response plots for the combined effects of process variables on removal efficiency. (a) and (b) effect of fluoride initial concentration and contact time; (c) and (d) effect of fluoride initial concentration and adsorbent dose at constant contact time; (e) and (f) effect contact time and adsorbent dose at constant fluoride initial concentration.

### 2.17.13 Effect of contact time

The Figs. 3a and 3e for As removal and Figs. 4a and 4e for  $F^-$  removal show the combined effect of contact time with initial concentration and adsorbent dose respectively. It is clear that, percentage removal increases with increase in contact time for both As (Figs. 3a and 3e) and  $F^-$  (Figs. 4a and 4e). This result is also revealed by the corresponding contour plots in Figs. 3b and 3f for As removal and in Figs. 4b and 4f for  $F^-$  removal respectively.

### 2.17.14 Optimization and validation of result

The investigation was carried out to find the optimum process variables that can maximize removal efficiency. In order to obtain the optimum condition, all the process variables were maintained within the range of experimental condition studied. Forty five (45) solutions were given by the statistical software based on the above conditions, from which solution number (1) with highest desirability was selected. To obtain the optimal condition for As and  $F^-$  removal with adsorption process, adsorbent dosage at the minimum level, initial As or  $F^-$  concentration at the maximum level and contact time in a range were set for maximum desirability (Figs. 5 and 6).

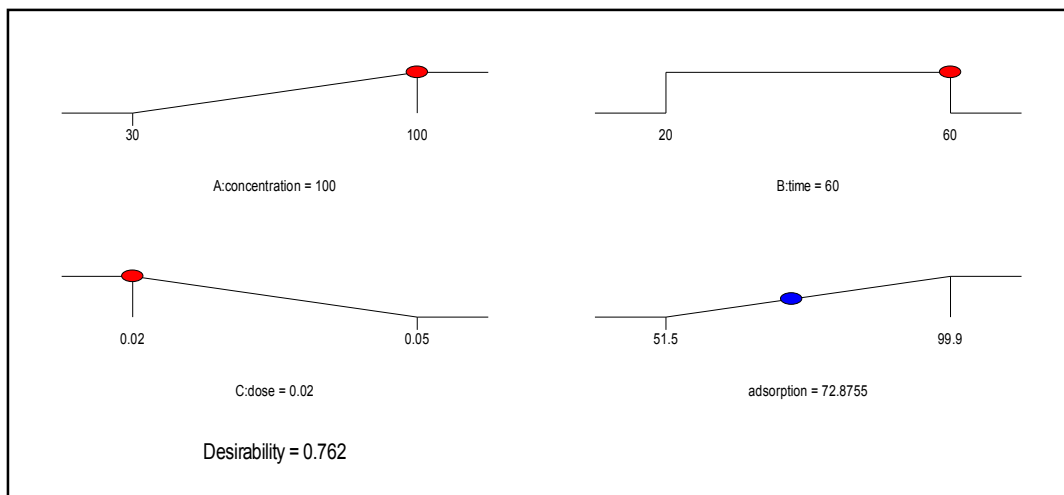


**Fig.5: Ramp desirability for optimization of arsenic adsorption**

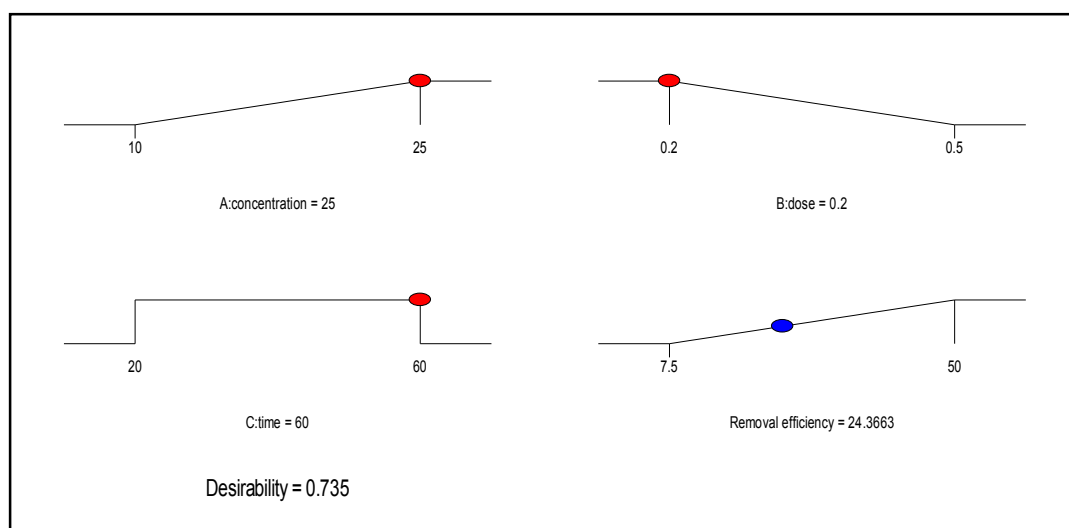


**Fig.6: Ramp desirability for optimization of fluoride adsorption**

After setting the above conditions, the optimum conditions were given by the statistical software. The best local maximum for As removal was found to be at initial ion concentration of  $100 \text{ mg L}^{-1}$ , adsorbent dosage of  $0.2 \text{ g/50 mL}$  and contact time 60 minutes with As removal of 72.8% and desirability of 0.76 (Fig. 5). Similarly, for  $\text{F}^{-}$  removal, the best condition for  $\text{F}^{-}$  removal was found to be at initial ion concentration of  $25 \text{ mg L}^{-1}$ , adsorbent dosage of  $0.2 \text{ g/50 mL}$  and contact time 60 minutes with  $\text{F}^{-}$  removal of 24.3% and desirability of 0.73 (Fig. 6).

The experiment with optimized process condition was carried out in triplicates and the average value of removal efficiency recorded (72.1% for As and 24.80% for  $\text{F}^{-}$ ) sufficiently agree with the predicted value. Hence, this validation confirms the adequacy of the developed quadratic model for removal efficiency.

#### 2.17.15 Adsorption kinetic study

The calculated kinetic parameters of pseudo-first-order and pseudo-second-order models are summarized in Table 6 and corresponding graphs are presented in supplementary document S8 and S9 respectively.

**Table 6: Kinetic parameters for adsorption rate expression of arsenic and fluoride removal**

Isotherm type	Isotherm parameters	Arsenic concentration (mg/L)				Fluoride concentration (mg/L)			
		6	30	65	100	5	10	17	25
Pseudo first order	$K_1$	0.010	0.012	0.002	0.003	0.004	0.003	0.0006	0.0001
	$R^2$	0.70	0.85	0.94	0.88	0.6527	0.5255	0.3541	0.2333
	$q_{cal}$	1.16	1.92	14.6	52.56	0.8055	1.1466	6.0833	17.52
Pseudo second order	$K_2$	0.03	0.02	0.005	0.006	0.02	0.01	0.002	0.002
	$R^2$	0.999	0.999	1.000	0.999	0.987	0.978	0.965	0.945
	$q_e$	9.8	17.5	26.1	28.65	6.8	10.45	10.87	9.55
Intra-particle	$K_{diff}$	0.328	0.642	1.065	1.291	0.227	0.383	0.443	0.430
	$R^2$	0.908	0.883	0.873	0.865	0.6305	0.5273	0.3637	0.2883
	C	5.16	8.92	8.49	5.39	3.58	5.32	3.53	1.79

The correlation coefficient for pseudo-second-order model for both As and  $F^-$  was found to be more than 0.999 and its calculated adsorption capacity at equilibrium ( $q_e$ ) values were in agreement with the experimental value. Consequently, adsorption of both As and  $F^-$  followed pseudo-second-order model. This result suggests that a chemisorption step might be rate determining in the As and  $F^-$  adsorption process (Cai et al. 2015). In chemisorption process, pseudo-second-order model is considered better than pseudo-first-order model because of the consideration of interaction between adsorbent and adsorbate (Massoudinejad et al. 2016).

#### 2.17.16 Adsorption isotherm

The calculated isotherm parameters for the Langmuir and Freundlich models for As and  $F^-$  removal are compared with previous literatures and are summarized in supplementary document S10. The graphical plots for Langmuir and Freundlich models for As and  $F^-$  removal are presented in supplementary document S11 and S12

respectively. It was found that the correlation coefficient of Langmuir equation is more than Freundlich isotherm. Therefore, the As and F<sup>-</sup> adsorption could be attributed to the presence of homogeneous surface active sites of activated biochar, and adsorption may take place in a monolayer adsorption manner. The Langmuir isotherm model describes the monolayer adsorption of the adsorbate on a homogeneous adsorbent surface. Consequently, the use of *S. ravannae* activated biochar to remove both As and F<sup>-</sup> from groundwater could be effective compared to other adsorbents (Kumar et al. 2011, Lunge et al. 2012).

## 11. Conclusions summarizing the achievements and indication of scope for future work:

### 3. Conclusion

The present study is probably the first effort to evaluate provenance, prevalence and associated health risk from As and F<sup>-</sup> co-occurrence in the aquifers of the Brahmaputra a tropical river floodplain (BFP). Groundwater of the BFP is mainly of Ca<sup>2+</sup>, Mg<sup>2+</sup>, HCO<sub>3</sub><sup>-</sup> type resulted from weathering of carbonate mineral. Reducing conditions were prevalent in the entire BFP and appeared to play a key role in release of As from Fe (hydr)oxides such as goethite and ferrihydrite via reductive hydrolysis.

Co-occurrence of As and F<sup>-</sup> in groundwater is a less than understood subject, moreover it is very difficult to replicate in laboratory the exact set of conditions found in natural settings. A sequential extraction procedure (SEP), batch desorption experiments and the concept of partition coefficient were applied on seven sediment samples from the Subansiri-Dikrong-Ranganadi River System (SDRS), a subset of the upper Brahmaputra floodplain (BFP), to understand leaching of arsenic (As) and fluoride (F<sup>-</sup>).

Findings from the present study showcase the behaviour of As and F<sup>-</sup> in reducing aquifers of the Brahmaputra Flood Plains (BFP). Significant correlation between total As and As extracted from fractions III and IV [Fe (hydr)oxides] suggests the main source of groundwater As was derived from Fe (hydr)oxide present in soils and sediments. Application of speciation and cluster analyses to understand co-contamination. Two contaminants were not found strongly correlated in their distribution. PO<sub>4</sub><sup>3-</sup>, HCO<sub>3</sub><sup>-</sup>, and H<sub>4</sub>SiO<sub>4</sub> enhance the mobility of both As and F<sup>-</sup>.

Regression analysis showed a weaker relationship between As and F<sup>-</sup> co-occurrence. Hierarchical cluster analysis (HCA) and principal component analysis (PCA) suggested reductive dissolution of Fe (hydr)oxides responsible for As release in the BFP, especially in the upper and lower BFP. Bicarbonate appeared to compete with As oxyanions for adsorption on positively charged surfaces leading to As release. Arsenic desorption in presence of PO<sub>4</sub><sup>3-</sup>, F<sup>-</sup> and HCO<sub>3</sub><sup>-</sup> at elevated pH appeared greatest in the upper BFP, suggesting the highest potential for co-occurrence. Co-occurrence, were mainly in isolated aquifers of the upper BFP owing to desorption of adsorbed As and F<sup>-</sup> from Fe (hydr)oxides at higher pH.

This study was novel in three ways; a) it studied As-F<sup>-</sup> co-contamination aspect which is not prevalent in recent literature, b) it looked at mitigation options from co-contaminated water and finally c) it evaluated the perception of indigenous people about the As problem and related issues.

Consequently, the risk computation by considering As ingestion through drinking water implied that the inhabitants of the area might confront higher toxic and carcinogenic risk in near future. Findings of the present study provide: (1) valuable baseline information for further studies on this topic; (2) a basis for better management of As and other coexisting toxic elements in groundwater; and (3) awareness and knowledge dissemination in the local language regarding public health issues and preventive measures.

Concurrently, Arsenic and Fluoride mitigation approaches has also been made by using green technology. Perennial grass based activated biochar was synthesized and characterized for possible application in both As and F<sup>-</sup> removal from water. Nanoscale rice husk biochar was also applied for remediation of fluoride from contaminated water. Experimental findings indicated the applied adsorbents could be a favourable, low cost and environment friendly material for simultaneous removal of As and F<sup>-</sup> from contaminated water.

Some of the keyfindings are:

- Isolated oxidized aquifers are also localities where co-occurrence could occur via pH-induced desorption, because such aquifers are drier with less recharge, conditions favorable for F<sup>-</sup> release.
- Saturation Index calculations revealed that gradual increase in the levels of As and F<sup>-</sup> in the near future a possibility, there is a high likelihood of the co-occurrence scenario developing into that of co-contamination.
- Non-cancer health risk from both As and F<sup>-</sup> was also highest in children, followed by adult males and females. Aquifer depth appeared to have an important influence on As and F<sup>-</sup> related health risks in the BFP

- Easier access to shallow aquifers with elevated levels of As is likely responsible for higher risk. As both arsenic and F<sup>-</sup> are poised to increase in the near future, the health implications are also appearing to get more serious.

## 12. S&T benefits accrued:

### i. List of Research publications

#### *List of Journal publications (International: 9)*

1. **R. Goswami**, M. Kumar N. Rengarajan, and P. Shea (2020). "Evaluation of Exposure and People's Perception of Health Risk due to Arsenic Contamination in Majuli (River Island), Assam, India", *Environmental Geochemistry and Health*. 42:443–460
2. **R. Goswami** (Joint first author) M. Kumar, and N. Awasthi (2019). "Provenance and Fate of Rare Earth Elements in the Sediment-Aquifers Systems of Majuli River Island, India," *Chemosphere*, 237, <https://doi.org/10.1016/j.chemosphere.2019.124477>
3. A.K. Patel, N. Das, **R. Goswami** and M. Kumar (2019). "Arsenic mobility and potential co-leaching of fluoride from the sediments of three tributaries of the Upper Brahmaputra floodplain, Lakhimpur, Assam, India." *Journal of Geochemical Exploration*, 203, 45-58.
4. **R. Goswami** and M. Kumar (2018). Removal of fluoride from aqueous solution using nanoscale rice-husk biochar. *Groundwater Sustainable Dev.* 7, 446–451
5. R. Saikia, **R. Goswami (Corresponding author)**, N. Bordoloi, K.K. Pant, M. Kumar and R. Katakati (2017). Removal of arsenic and fluoride from aqueous solution by biomass based activated biochar: Optimization through response surface methodology. *J. Environ. Chem. Eng.* 5, 5528-5539.
6. M. Kumar, A.K. Patel, A. Das, P. Kumar, **R. Goswami**, J.P. Deka and N. Das (2017). Hydrogeochemical controls on mobilization of arsenic and associated health risk in Nagaon district of the central Brahmaputra Plain, India *Environmental Geochemistry and Health*, 39(1), 161-178.
7. M. Kumar, N. Das, K. P. Sarma, **R. Goswami**, AL. Ramanathan, P. Bhattacharya (2016). "Coupling fractionation and batch desorption to understand arsenic and fluoride co-contamination in the aquifer system". *Chemosphere* 164:657-667

8. M. Kumar, A. Das, N. Das, **R. Goswami** and U.K. Singh (2016). “Co-occurrence perspective of arsenic and fluoride in the groundwater of Diphu, Assam, North-eastern India”, *Chemosphere*, 150, 227-238.
9. **R. Goswami**, J. Shim, S. Deka, D. Kumar R. Kataki and M. Kumar (2016). “Characterization of cadmium removal from aqueous solution by biochar produced from Ipomoea Fistulosa at different pyrolytic temperatures”. *Ecological Engineering*, 97; 444-451

***Book Chapters: Three***

1. **R. Goswami** and M. Kumar. Inorganic arsenic exposure and children at risk in Majuli- the most thickly populated river island of the world. (2016). CRC press(**Taylor & Francis**), Pp. 460-461, ISBN 9781138029415.
2. M. Kumar, AL Ramanathan, S. Chidambaram, **R. Goswami**(2015) “Analytical technique and methods of water reuse options” *In: Urban Water Reuse Handbook (UWRH)*, Edition: 1st Edition, IAHS Publication, ISBN: 9781482229141. pp163-174
3. N. Das, L. Khanikar, R. Shah, A. Das, **R. Goswami**, M. Kumar and K.P. Sarma, (2015). Problem, Perspective and Challenges of Arsenic Contamination in the Groundwater of Brahmaputra Flood Plains and Barak Valley Regions of Assam, India. *In: Safe and Sustainable Use of Arsenic-Contaminated Aquifers in the Gangetic Plain: A Multidisciplinary Approach*. Springer International Publishing, Cham, Switzerland. ISBN: 978-3-319-16124-2. pp 69-86

***List of papers presented in conference/ seminar: Seven***

1. **R. Goswami**, A.K. Patel, , and M.Kumar. Evaluation of groundwater quality with emphasis on Arsenic and fluoride concentration in Guwahati: Economic hub of Northeast India. Published in Conference Proceeding of **6<sup>th</sup> International Symposium on “Advances in Civil and Environmental Engineering Practices for Sustainable Development”** (ACEPS-2018), pp: 87-91, ISSN: 2279-1329, Galle, Sri Lanka, Mar, 15, 2018
2. **R. Goswami**, R. Thakur, M. Kumar. “Co-contamination perspective of arsenic with fluoride and associated health risk in Lakhimpur district in the upper Brahmaputra floodplain”. **Oral presentation** in the **International Seminar on Land And Water Issues in South East Asia: Status, Challenges and Opportunities**. held during 18-20 Jan, 2018 at NERIWALM, Tezpur, Assam.

3. **R. Goswami**, M. Kumar “Exposure And Health Risk Assessment Of Inorganic Arsenic Intake Through Groundwater Drinking Pathway- A Study From Majuli, The Largest Inhabited river Island of the World” National Symposium on Environment (NSE-20) held during 13-15 December, 2018 at IIT Gandhinagar, Gujarat.
4. **R. Goswami**, M. Kumar, A.K. Patel, A. Das, (2016). Understanding of Arsenic contamination in the southern floodplain of Brahmaputra River, Assam, North-east India through Major ion chemistry, Speciation modeling, Statistical analyses and Health Risk Assessment. **Sixth International Groundwater Conference (IGWC-2015)**, SRM University, Chennai Tamil Nadu, India and Association of Global Groundwater Scientists (AGGS), India.
5. **R. Goswami**, M. Kumar. “Removal of Fluoride from Drinking Water Using a Plant Derived Nano Adsorbent”. *Oral presentation* in the **International Ground Water Conference( IGWC, 2015)** held during 11-13 Feb, 2016 at SRM University in Chennai.
6. **R. Goswami**, A. Das and M. Kumar (2015). Geochemistry of trace and rare-earth elements in Holocene sediments of the largest riverine Island of Majuli, Assam, India, **National seminar on “Past and Present Geochemical Processes - Impacts on Climate Change**, Jawaharlal Nehru University (JNU), New Delhi.

**ii. Manpower trained on the project**

- a) Research Scientists or Research Associates: NA
- b) No. of Ph.D. produced: NA
- c) Other Technical Personnel trained: 2 MSc students trained

iii. Patents taken, if any : NA

### 13. Financial Position:

No	Financial Position/ Budget Head	Funds Sanctioned	Expenditure	% of Total cost
I	Salaries/ Manpower costs	1911000	1765000	60
II	Equipment	500000	500000	15
III	Supplies & Materials	190000	1,96,195	6
IV	Contingencies	150000	50719	6
V	Travel	100000	100000	3
VI	Overhead Expenses	300000	300000	10
VII	Others, if any(Interest earned)	11914		
	<b>Total</b>	3151000	2911914(including interest)	<b>100%</b>

### 14. Procurement/ Usage of Equipment

a)

S No	Name of Equipment	Make/Model	Cost (FE/ Rs)	Date of Installation	Utilisation Rate (%)	Remarks regarding maintenance/ breakdown
1	Fluoride Ion Selective Electrode (ISE)	Thermo Scientific	332000	06/08/15	100	Proper care is taken and in fully functional condition
2	UV Visible Spectrophotometer	Thermo Scientific	168000	12/12/15	100	

### b) Plans for utilizing the equipment facilities in future

The equipments will be kept in the Dept of Environmental Science, Tezpur University and will be used for the project works of the master's students and research scholars.

Name and Signature with Date

a. Ritusmita Goswami

(Principal Investigator)

b. \_\_\_\_\_

(Co-Investigator)

## Reference

Aleksiyev V. A; Kochnova L. N; Cherkasova E. V and Tyutyunnik O.A (2010) Possible Reasons for Elevated Fluorine Concentrations in Groundwaters of Carbonate Rocks. ISSN 0016\_7029, *Geochemistry International* 48, No. 1, 68–82.

Amentia M.A and Segovia N. (2006) Arsenic and Fluoride in the groundwater of Mexico.

*Environ Geochem Health* 30: 345–353.

Anawar Hossain M; Akai Junji; Sakugawa Hiroshi (2004) Mobilization of arsenic from subsurface sediments by effect of bicarbonate ions in groundwater. *Chemosphere*, 54, 753–762.

Appelo C.A.J ; Weiden Van Der ; Tournassat and L Charlet (2002) Surface Complexation of Ferrous Iron and Carbonate on Ferrihydrite and the Mobilization of Arsenic. *Environ. Sci. Technol*, 36, 3096-3103.

Bhattacharya Prosun; Hasan M. Aziz; Sracek Ondra; Smith Euan; Ahmed K. Matin; Broßmsen Mattias von; Huq S. M. Imamul and Naidu Ravi(2009) Groundwater chemistry and arsenic mobilization in the Holocene flood plains in south-central Bangladesh. *Environ Geochem Health*, 31:23–43.

Chakraborti Dipankar; Singh E. Jayantakumar; Das Bhaskar; Shah Babar Ali; Hossain M. Amir; Nayak Bishwajit; Ahamed Sad and Singh N. Rajmuhon (2007) Groundwater arsenic contamination in Manipur, one of the seven North-Eastern Hill states of India: a future danger. *Environ Geol*, 56:381–390.

De la Sota M; Puche R; Rigalli A; Fernandez LM; Benassatti S and Boland R (1997) Changes in bone mass and in glucose homeostasis in subjects with high spontaneous fluoride intake. *Medicina(B Aires)*57(4):417-20.

Deshmukh, A. N. Valadaskar PM, Malpe DB (1995). Fluoride in environment: a review.

*Gondwana Geol. Mag.* 9, 1–20.

Dutta Robin K; Das Babulal; Talukdar Jitu; Sarma Surashree; Gohain Biren; Das Himangshu B and Das Subhash C (2003) Fluoride and other inorganic constituents in groundwater of Guwahati, Assam, India. *Current Science*, 85, 5-10.

Edmunds, W.M. and Smedley, P.L. (2005) Fluorine in natural waters - occurrence, controls and health aspects. In, O. Selnius (ed.) *Medical Geology Reference - Earth Science Information in Support of Public Health Protection*. Academic. 301-329.

Harvey Charles F; Ashfaque Khandaker N; Yu Winston; Badruzzaman A.B.M; Ali M. Ashraf; Oates Peter M; Michael Holly A; Neumann Rebecca B; Beckie Roger; Islam Shafiqul; Ahmed M. Feroze (2006) Groundwater dynamics and arsenic contamination in Bangladesh. *Chemical Geology* 228, 112–136.

Hoang Thi Hanh; Bang Sunbaek; Kim Kyoung-Woong; Nguyen My Hoa and Dang Duy Minh (2010) Arsenic in groundwater and sediment in the Mekong River delta, Vietnam. *Environmental Pollution* 158, 2648-2658.

Kerro M. L; Vieiro A. P and Machado G (2007) The fluoride in the groundwater of Guarani Aquifer System: the origin associated with black shales of Parana' Basin. *Environ Geol* 55, 1219–1233.

Kim, S. Y. (2001) Hydrogeochemical, geostatistical and thermodynamical studies on deep thermal groundwater, Korea. Unpub. Ph.D thesis, Korea Univ.

Kinniburgh D. G and Smedley P. L (2001) Arsenic contamination of groundwater in Bangladesh. BGS Technical Report WC/00/19. Keyworth, British Geological Survey & Department of Public Health Engineering.

Kumar Manish; Kumar Pankaj; Ramanathan A.L; Bhattacharya Prosun; Thunvik Roger; Kumar Umesh; Tsujimura M and Sracek Ondra (2010) Arsenic enrichment in groundwater in the middle Gangetic Plain of Ghazipur District in Uttar Pradesh, India. *Journal of Geochemical Exploration* 105 83–94.

Li Xiangquan; Hou Xinwei; Zhou Zhichao and Liu Lingxia (2010) Geochemical provenance and spatial distribution of fluoride in groundwater of Taiyuan basin, China. *Environ Earth Sci* 62, Number 8, 1635-1642.

Mamatha, P and Rao Sudhakar M (2009) Geochemistry of fluoride rich groundwater in Kolar and Tumkur Districts of Karnataka. *Environ Earth Sci* 61:131–142.

Moghaddam, Asghar Asghari and Fijani, Elham (2007) Distribution of fluoride in groundwater of Maku area, northwest of Iran. *Environ Geol* 56: 281–287.

Shah Babar Ali (2010) Arsenic-contaminated groundwater in Holocene sediments from parts of Middle Ganga Plain, Uttar Pradesh, India. *Current Science* 98, no. 10.

Singh A.K (2006) Chemistry of arsenic in groundwater of Ganges–Brahmaputra river basin. *Current Science* 91, 5-10.

Smedley P. L. and Kinniburgh D. G. (2002) A review of the source, behaviour and distribution of arsenic in natural waters. *Applied Geochemistry* 17, 517-568.

Subba Rao, N (2010) High-fluoride groundwater. *Environ Monit Assess* 176, Number 1-4, 637-645.

Sujatha, D. (2003) Fluoride levels in the groundwater of the south-eastern part of Ranga Reddy district, Andhra Pradesh, India. *Environ. Geol.* 44, 587–591.

Tekle-Haimanot, R., Melaku, Z., Kloos, H., Reimann, C., Fantaye, W., Zerihun, L., and Bjorvatn, K. (2006): The geographic distribution of fluoride in surface and groundwater in Ethiopia with an emphasis on the Rift Valley, *Sci. Total Environ* 367, 182–190.

UNICEF, 2000 Global Water Supply and Sanitation Assessment 2000 Report

Yun, S. T., Chae, G. T., Koh, Y. K., Kim, S. R., Choi, B. Y., Lee, B. H. and Kim, S. Y. (1998a) Hydrogeochemical and environmental isotope study of groundwaters in the Pungki area. *J. Kor.Soc. Groundwater Environ* 5, 177–191.

Yun, S. T., Koh, Y. K., Choi, H. S., Youm, S. J. and So, C. S. (1998b) Geochemistry of geothermal waters in Korea: environmental isotope and hydrochemical characteristics. II. Jungwon and Munkyeong areas. *Econ. Environ. Geol* 31, 201–213.

Yun, S. T.; Chae, Gi Tak; Kwon, Man Jae; Kim, Yi Seop And Mayer, Bernhard (2006) Batch dissolution of granite and biotite in water: Implication for fluorine geochemistry in groundwater. *Geochemical Journal* Vol. 40, 95- 102.

Chen, K.Y., Liu, T.K., 2007. Major factors controlling arsenic occurrence in the groundwater and sediments of the Chianan Coastal Plain, SW Taiwan. *Terr. Atmos. Ocean. Sci.* 18, 975–994. [https://doi.org/10.3319/TAO.2007.18.5.975\(TT\)](https://doi.org/10.3319/TAO.2007.18.5.975(TT))

Critto, A., Carlon, C., Marcomini, A., 2003. Characterization of contaminated soil and groundwater surrounding an illegal landfill (S. Giuliano, Venice, Italy) by principal component analysis and kriging. *Environ. Pollut.* 122, 235–244. [https://doi.org/10.1016/S0269-7491\(02\)00296-8](https://doi.org/10.1016/S0269-7491(02)00296-8)



## Annexure-III

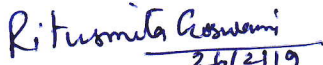
**CONSOLIDATED UTILIZATION CERTIFICATE  
FOR THE FINANCIAL YEAR (20<sup>th</sup> JUNE, 2014 TO 31<sup>st</sup> MARCH, 2018)**

1.	Title of the Project/ Scheme: "Understanding of Arsenic phase distribution and co-contamination perspective with fluoride in the Brahmaputra flood plains"	
2.	Name of the Institution	Tezpur University
3.	Principal Investigator	Dr. Ritusmita Goswami
4.	Deptt. of Science & Technology letter No. & date sanctioning the project	SR/FTP/ES-27/2013 Dated 20/02/2014
5.	Head of account as given in the original sanction letter	Capital Budget Head & General Budget Head
6.	Amount brought forward from the previous financial year quoting DST letter No. and date in which the authority to carry forward the said amount was given	I. Amount: NIL II. Letter No: NA III. Date: NA
7.	Amount received during the financial Year (Please give No. & date) of DST's sanction letter for the amount	I. Amount: Rs. 29,00,000 II. Letter No. SERB/FTP/ES-27/2013 III. Date: 20/02/2014
8.	Total amount that was available for expenditure (including interest Rs. 11,914) during the financial year (S.No. 6+7+8)	Rs. 29,11,914
9.	Actual expenditure (excluding commitments) incurred during the financial year (Upto 31 <sup>st</sup> March 2018)	Rs. 29,11,914
10.	Balance amount available at the end of the financial year	Rs. NIL
11.	Unspent balance refunded if any (Please give details of cheque, Demand draft No. etc.)	Rs. NIL
12.	Amount to be carried forward to the next financial year (if applicable)	Rs. NIL

  
 Finance Officer  
 Tezpur University

## UTILIZATION CERTIFICATE

Certified that out of Rs. 29,11,914/- of grants-in-aid sanctioned and received during the year 2014- 2017 in favour of Registrar, Tezpur University, Tezpur under the Department of Science & Technology Letter No. SR/FTP/ES-27/2013 dated 20/02/2014 and Rs. NIL on account of unspent balance of previous year, a sum of Rs. 29,11,914 has been utilized for the purpose of Project for which it was sanctioned and that the balance of Rs. NIL remaining unutilized at the end of the year.

  
Signature of Principal  
Investigator  
with date

(TO BE FILLED IN BY DST)

  
Signature of Registrar/  
Accounts Officer  
with date  
*Finance Officer*  
*Tezpur University*

  
Signature of Head  
of the Institute Date  
*Registrar*  
*Tezpur University*

2. Certified that I have satisfied myself that the conditions on which the grants-in-aid was sanctioned have been fulfilled/ are being fulfilled and that I have exercised the following checks to see that the money was actually utilized for the purpose for which it was sanctioned: -

Kinds of checks exercised.

- 1.
- 2.
- 3.

Signature  
Designation  
Date

**REQUEST FOR ANNUAL INSTALMENT WITH UP-TO-DATE STATEMENT OF EXPENDITURE**

1. Sanction Order No and date: **SR/FTP/ES-27/2013 20/02/2014**
2. Total Project Cost: **25,00,000/-**
3. Revised Project Cost: **31,51,000**  
(if applicable)
4. Date of Commencement: **20.06.2014**

Statement of Expenditure: **20<sup>th</sup> June, 2014 to 31<sup>st</sup> March, 2018**  
(Month wise expenditure incurred during current financial year)

<b>Month &amp; year</b>	<b>Expenditure incurred/ committed</b>
20 <sup>th</sup> June, 2014 to 31 <sup>st</sup> March 2018	<b>2911914 /-</b>

5. Grant received in each year:
  - a. 1<sup>st</sup> Year: 12,00,000/-
  - b. 2<sup>nd</sup> Year: 9,00,000/-
  - c. 3<sup>rd</sup> Year: 2,00,000/-
  - d. 3<sup>rd</sup> Year: 6,00,000/-
  - e. Interest, if any: 11,914
  - f. Total (a+b+c+d):29,11,914/-

**Consolidated Statement of Expenditure**  
(20<sup>th</sup> June, 2014 to 31<sup>st</sup> March, 2018)

Sr No	Sanctioned Heads	Funds Allocated (indicate sanctioned or revised)	Expenditure Incurred (20 <sup>th</sup> June, 2014 to 31 <sup>st</sup> March, 2015)	Expenditure Incurred (1 <sup>st</sup> April, 2015 to 31 <sup>st</sup> March, 2016)	Expenditure Incurred (1 <sup>st</sup> April, 2016 to 31 <sup>st</sup> March, 2017)	Expenditure Incurred (1 <sup>st</sup> April, 2017 to 31 <sup>st</sup> March, 2018)*	Total Expenditure	Due as on (31 <sup>st</sup> March) as per allocation	Requirement of Funds
1.	Manpower costs	1911000	540000	55000	660000	510000	1765000	146000	146000
2.	Consumables	190000	90419	105776	Nil		1,96,195	-6195	-6195
3.	Travel	100000	Nil	Nil	27596	72404	100000	Nil	Nil
4.	Contingencies	150000	10099	11645	11379	17596	50719	99281	99281
5.	Others, if any		Nil	Nil					Nil
6.	Equipment	500000	Nil	500000			500000		Nil
7.	Overhead expenses	300000	62500	37500	Nil	200000	300000	Nil	Nil
8.	Interest	11914							
9.	Total (Rs)	3151000	703018	709921	698975	800000	2911914	239086	239086

\*Project was ended on 19<sup>th</sup> March 2018

Fund allocated: 31,51,000.00

Fund released: 29,00,000.00

Interest earned: 11,914.00

Fund utilized: 29,11,914.00 (including earned interest)

Actual balance in hand: Nil

Fund due: 2,39,086.00

Name and Signature of Principal Investigator:

Date:

*RITUSMITA CROSWAMI*

26/2/19

Signature of Competent financial authority: \_\_\_\_\_  
(with seal) Date: \_\_\_\_\_

*Finance Officer*  
*Tezpur University*

\* DOS – Date of Start of project

Note :

1. Expenditure under the sanctioned heads, at any point of time, should not exceed funds allocated under that head, without prior approval of DST i.e. Figures in Column (VIII) should not exceed corresponding figures in Column (III)
2. Utilisation Certificate (Annexure III) for each financial year ending 31<sup>st</sup> March has to be enclosed along with request for carry-forward permission to the next financial year.

## Annexure-III

**UTILIZATION CERTIFICATE  
FOR THE FINANCIAL YEAR (20<sup>th</sup> June, 2014 TO 31<sup>ST</sup> MARCH, 2015)**

1.	Title of the Project/ Scheme: "Understanding of Arsenic phase distribution and co-contamination perspective with fluoride in the Brahmaputra flood plains"	
2.	Name of the Institution	Tezpur University
3.	Principal Investigator	Dr. Ritusmita Goswami
4.	Deptt. of Science & Technology letter No. & date sanctioning the project	SR/FTP/ES-27/2013 Dated 20/02/2014
5.	Head of account as given in the original sanction letter	Capital Budget Head & General Budget Head
6.	Amount brought forward from the previous financial year quoting DST letter No. and date in which the authority to carry forward the said amount was given	I. Amount: Rs NIL II. NA III. NA
7.	Amount received during the financial Year (Please give No. & date) of DST's sanction letter for the amount	I. Amount: 12,00,000/- II. Letter No. SR/FTP/ES-27/2013 III. Date: 20/02/2014
8.	Total amount that was available for expenditure (excluding commitments) during the financial year (S.No. 6+7)	Rs. 12,00,000/- + 11914/- (Interest of FY 2014 -15) = 12,11,914/-
9.	Actual expenditure (excluding commitments) incurred during the financial year (Upto 31st March)	Rs. 7,03,018/-
10.	Balance amount available at the end of the financial year	Rs. 5,08,896/- (including interest)
11.	Unspent balance refunded if any (Please give details of cheque, Demand draft No. etc.)	Rs. Nil
12.	Amount to be carried forward to the next financial year (if applicable)	Rs. 5,08,896/-

  
 Finance Officer  
 Tezpur University

## UTILIZATION CERTIFICATE

Certified that out of Rs. 12,00,000/- of grants-in-aid sanctioned during the year 20<sup>th</sup> June, 2014 to 31<sup>st</sup> March, 2015 in favour of Registrar, Tezpur University, Tezpur under the Department of Science & Technology Letter No. SR/FTP/ES-27/2013 dated 20/02/2014 and Rs. NIL on account of unspent balance of previous year, a sum of Rs. 7,03,018/- has been utilized for the purpose of Project for which it was sanctioned and that the balance of Rs. 5,08,896/- ( 4,96,982/- + 11914/- as interest) remaining unutilized at the end of the year will be adjusted towards the next year i.e. 2015 -2016.

  
Signature of Principal  
Investigator  
with date

(TO BE FILLED IN BY DST)

  
Signature of Registrar/  
Accounts Officer  
with date  
*Finance Officer  
Tezpur University*

  
Signature of Head  
of the Institute Date  
*Registrar  
Tezpur University*

2. Certified that I have satisfied myself that the conditions on which the grants-in-aid was sanctioned have been fulfilled/ are being fulfilled and that I have exercised the following checks to see that the money was actually utilized for the purpose for which it was sanctioned: -

Kinds of checks exercised.

- 1.
- 2.
- 3.

Signature  
Designation  
Date

## Annexure-III

**UTILIZATION CERTIFICATE  
FOR THE FINANCIAL YEAR (1<sup>ST</sup> APRIL, 2015 TO 31<sup>ST</sup> March, 2016)**

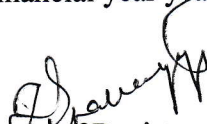
1.	Title of the Project/ Scheme: "Understanding of Arsenic phase distribution and co-contamination perspective with fluoride in the Brahmaputra flood plains"	
2.	Name of the Institution	Tezpur University
3.	Principal Investigator	Dr. Ritusmita Goswami
4.	Deptt. of Science & Technology letter No. & date sanctioning the project	SR/FTP/ES-27/2013 Dated 20/02/2014
5.	Head of account as given in the original sanction letter	Capital Budget Head & General Budget Head
6.	Amount brought forward from the previous financial year quoting DST letter No. and date in which the authority to carry forward the said amount was given	I. Amount: (Rs 4,96,982/- + 11914/- as Interest for FY 2014-15) = 5,08,896 II. Letter No. NA III. Date: NA
7.	Amount received during the financial Year (Please give No. & date) of DST's sanction letter for the amount	I. Amount: NIL II. Letter No. NA III. Date: NA
8.	Total amount that was available for expenditure (excluding commitments) during the financial year (S. No. 6+7)	Rs. 5,08,896/- (Interest Nil in the FY 2015- 16)
9.	Actual expenditure (excluding commitments) incurred during the financial year (Up to 31st March)	Rs. 7,09,921/-
10.	Balance amount available at the end of the financial year	Rs. (-)2,01,025/- (Excess expenditure)
11.	Unspent balance refunded if any (Please give details of cheque, Demand draft No. etc.	Rs. (-)2,01,025/-
12.	Amount to be carried forward to the next financial year (if applicable)	Rs. Nil

  
 Finance Officer  
 Tezpur University

## UTILIZATION CERTIFICATE

Certified that out of Rs. NIL of grants-in-aid sanctioned during the year 2015 -2016 in favour of Registrar, Tezpur University, Tezpur under the Department of Science & Technology Letter No. NA dated NA and Rs. 5,08,896/- on account of unspent balance of previous year, a sum of Rs. 7,09,921/- has been utilized for the purpose of Project for which it was sanctioned and that the Excess Expenditure of Rs. (-)2,01,025/- at the end of the year will be adjusted towards the current financial year year i.e. 2015 -2016.

  
Signature of Principal Investigator  
with date

  
Signature of Registrar/  
Accounts Officer  
with date  
*Finance Officer*  
*Tezpur University*

  
Signature of Head  
of the Institute Date  
*Registrar*  
*Tezpur University*

(TO BE FILLED IN BY DST)

2. Certified that I have satisfied myself that the conditions on which the grants-in-aid was sanctioned have been fulfilled/are being fulfilled and that I have exercised the following checks to see that the money was actually utilized for the purpose for which it was sanctioned: -

Kinds of checks exercised.

- 1.
- 2.
- 3.

Signature  
Designation  
Date

## Annexure-III

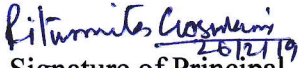
**UTILIZATION CERTIFICATE**  
**FOR THE FINANCIAL YEAR (1<sup>ST</sup> APRIL, 2016 TO 31<sup>ST</sup> March, 2017)**

1.	Title of the Project/ Scheme: "Understanding of Arsenic phase distribution and co-contamination perspective with fluoride in the Brahmaputra flood plains"	
2.	Name of the Institution	Tezpur University
3.	Principal Investigator	Dr. Ritusmita Goswami
4.	Deptt. of Science & Technology letter No. & date sanctioning the project	SR/FTP/ES-27/2013 Dated 20/02/2014
5.	Head of account as given in the original sanction letter	Capital Budget Head & General Budget Head
6.	Amount brought forward from the previous financial year quoting DST letter No. and date in which the authority to carry forward the said amount was given	I. Amount: Rs. (-)212939 (Negative balance) II. Letter No. NA  III. Date: NA
7.	Amount received during the financial Year (Please give No. & date) of DST's sanction letter for the amount	I. <b>Total Amount: Rs.11,00,000 (2 installments)</b> II. Letter No. SERB/F/3189(Rs.9,00,000) III. Date: 19/08/2016 IV. Letter No. SERB/F/9749(Rs.2,00,000) V. Date: 22/03/2017
9.	Total amount that was available for expenditure (excluding commitments) during the financial year (S. No. 6+7)	Rs. 8,98,975
10.	Actual expenditure (excluding commitments) incurred during the financial year (Up to 31st March)	Rs. 6,98,975
11.	Balance amount available at the end of the financial year	Rs.2,00,000
12.	Unspent balance refunded if any (Please give details of cheque, Demand draft No. etc.	Rs. Nil
13.	Amount to be carried forward to the next financial year (if applicable)	Rs. 2,00,000

  
 Finance Officer  
 Tezpur University

## UTILIZATION CERTIFICATE

Certified that out of Rs. 11,00,000 of grants-in-aid sanctioned during the year 2016 -2017 in favour of Registrar, Tezpur University, Tezpur under the Department of Science & Technology (Letter No. SERB/F/3189 dated 19/08/2016 and Letter No. SERB/F/9749 dated 22/03/2017) and Rs. (-)2,12,939 (excess expenditure) on account of unspent balance of previous year, plus Rs. 11914 as interest generated from the project fund, a sum of Rs. 6,98975 has been utilized for the purpose of Project for which it was sanctioned and that the Excess Expenditure of Rs.2,00,000 at the end of the year will be adjusted towards the next financial year year i.e. 2017 -2018.

  
Signature of Principal  
Investigator  
with date

  
Signature of Registrar/  
Accounts Officer  
with date  
*Finance Officer  
Tezpur University*

  
Signature of Head  
of the Institute Date  
*Registrar  
Tezpur University*

(TO BE FILLED IN BY DST)

2. Certified that I have satisfied myself that the conditions on which the grants-in-aid was sanctioned have been fulfilled/are being fulfilled and that I have exercised the following checks to see that the money was actually utilized for the purpose for which it was sanctioned: -

Kinds of checks exercised.

- 1.
- 2.
- 3.

Signature  
Designation  
Date

## Annexure-III

**UTILIZATION CERTIFICATE  
FOR THE FINANCIAL YEAR (1<sup>ST</sup> APRIL, 2017 TO 31<sup>ST</sup> Mar, 2018)**

1.	Title of the Project/ Scheme: "Understanding of Arsenic phase distribution and co-contamination perspective with fluoride in the Brahmaputra flood plains"	
2.	Name of the Institution	Tezpur University
3.	Principal Investigator	Dr. Ritusmita Goswami
4.	Deptt. of Science & Technology letter No. & date sanctioning the project	SR/FTP/ES-27/2013 Dated 20/02/2014
5.	Head of account as given in the original sanction letter	Capital Budget Head & General Budget Head
6.	Amount brought forward from the previous financial year quoting DST letter No. and date in which the authority to carry forward the said amount was given	I. Amount: 2,00,000 II. Letter No: SR/FTP/ES-27/2013  III. Date: 29/09/2017
7.	Amount received during the financial Year (Please give No. & date) of DST's sanction letter for the amount	I. Amount: Rs. 6,00,000 II. Letter No. SERB/F/6234/2017-2018 III. Date: 29/09/2017
8.	Total amount that was available for expenditure (excluding commitments) during the financial year (S.No. 6+7+8)	Rs. 8,00,000
9.	Actual expenditure (excluding commitments) incurred during the financial year (Upto 31 <sup>st</sup> Dec 2017)	Rs.8,00,000
10.	Balance amount available at the end of the financial year	Rs. NIL
11.	Unspent balance refunded if any (Please give details of cheque, Demand draft No. etc.	Rs. NIL
12.	Amount to be carried forward to the next financial year (if applicable)	Rs. NIL

  
 Finance Officer  
 Tezpur University

## UTILIZATION CERTIFICATE

Certified that out of Rs. 8,00,000/- of grants-in-aid sanctioned and received during the year 2017- 2018 in favour of Registrar, Tezpur University, Tezpur under the Department of Science & Technology Letter No. SR/FTP/ES-27/2013 dated 29/09/2017 and Rs. NIL on account of unspent balance of previous year, a sum of Rs. 8,00,000 has been utilized for the purpose of Project for which it was sanctioned and that the balance of Rs. NIL remaining unutilized at the end of the year will be adjusted towards the current financial year i.e. 2017 -2018.

*Ritumita Goswami*  
26/12/19  
Signature of Principal  
Investigator  
with date

(TO BE FILLED IN BY DST)

*[Signature]*  
Signature of Registrar/  
Accounts Officer  
with date  
*Finance Officer*  
*Tezpur University*

*[Signature]*  
Signature of Head  
of the Institute Date  
*Registrar*  
*Tezpur University*

2. Certified that I have satisfied myself that the conditions on which the grants-in-aid was sanctioned have been fulfilled/ are being fulfilled and that I have exercised the following checks to see that the money was actually utilized for the purpose for which it was sanctioned: -

Kinds of checks exercised.

- 1.
- 2.
- 3.

Signature  
Designation  
Date